Journal of Membranes and Materials v(i) pp-pp (YYYY)
Received Month Year / Revised Month Year / Accepted Month Year

Journal of Membranes and Materials

https://ejournal2.undip.ac.id/index.php/jmm

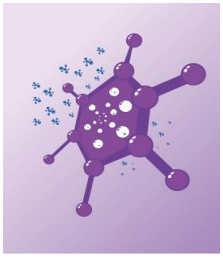

Hydrophilic Modification of PVDF Membrane: a Review

Herlambang Abriyanto[1,2*]

[1]*Department of Chemical Engineering, Faculty of Engineering, Diponegoro University, INDONESIA 50275*
[2]*Membrane Research Center (Mer-C), Diponegoro University, INDONESIA 50275*

**Corresponding author : herlambang.abri@gmail.com*

Abstract. The key challenges faced by using membranes in carrying out this water treatment process are increasing filtering efficiency and reducing the cost of water treatment. PVDF is one of the most widely used membrane materials, and its outstanding properties, such as high mechanical strength, thermal stability, chemical resistance and hydrophobicity, have received a great deal of attention from researchers and manufacturers in recent years. However, the strong hydrophobic properties of pure PVDF membranes, when handling aqueous solutions containing some natural organic and colloidal materials which are susceptible to deposition and absorption to the membrane surface, often lead to low water permeability and fast fouling. There are many methods of modification to change the properties of the antifouling membrane surface by physical modification (coating, mixing and use of composite membranes) and chemical modification (polymer functionalization, plasma processing and graft polymerization). Several methods of increasing the hydrophilicity value of membranes, such as surface coating, surface grafting and plasma polymerization, will be presented in this review paper.

Keywords: fouling, hydrophilicity, membrane, modification, PVDF

1. Introduction

It is not possible to ignore the rising number of people on earth, which has an effect on the state and balance of the current ecosystem. One of them is the state of water that is increasingly contaminated and unsanitary to use in the world. Humans are now competing to build technologies for water treatment so that it can be reused. This technology can be an alternative option to replace other separation technologies or even be used with other separation technologies in an integrated way, since there are many important advantages of using membranes for industrial processes, such as no phase change or chemical addition, easy to update modular, easy to operate, relatively low energy consumption, etc.

In various fields such as water treatment, gas purification (Zhang et al., 2013), food processing (Charcosset, 2009), the pharmaceutical industry (Zaviska et al., 2013) and environmental conservation, membrane technology has therefore been widely used.However, of the many uses of this membrane technology, water treatment and wastewater treatment are the ones that most utilize membrane technology in overcoming these problems.In carrying out this method of water treatment, increasing filtering efficiency and reducing water treatment costs are the key challenges facing the use of membranes.

The sieving method with a moving force in the form of pressure is the method used in the process of filtering water with a membrane. Pressure-activating membrane processes are categorized into membrane microfiltration (MF), UF, nanofiltration (NF), reverse osmosis (RO) and are based on variations in membrane pore size. Fouling is the key issue that is often faced in the filtering process, apart from the difficulty of increasing the filtration performance of membranes. Fouling is the blockage by dirt or contaminants of membrane pores present in the feed solution to be filtered. Membrane impurities are recognized as a key element as they both temporarily and permanently reduce membrane flux. Membrane impurities are considered a major problem as they both temporarily and permanently reduce membrane flux. Therefore, in addition to mechanical, thermal and chemical properties, many membrane researchers worldwide are competing to conduct research to enhance the efficiency of membranes that have strong anti-fouling properties. Properties of membranes. Better still. The engineering process in improving membrane performance can be carried out in various ways, including modifying the operating conditions of the membrane to reduce fouling and increase the flux value. Using a good membrane material, modifying the constituent material of the membrane, adding compounds that have good antifouling properties.

At present, almost all membranes used in industrial processes are made of inorganic materials and / or organic polymers. Examples of organic polymers include PVDF, polysulfone (PSF), poly (ether sulfone) (PES), polyacrylonitrile (PAN), polyamide (PA), polyimide (PI) and polytetrafluoroethylene (PTFE). Of these, PVDF is one of the most commonly used membrane materials and, in recent years, has received a great deal of attention from researchers and manufacturers with respect to its outstanding properties, such as high mechanical strength, thermal stability, chemical resistance and hydrophobicity. (Liu et al., 2011). However, the strong hydrophobic nature of pure PVDF membranes always causes low water permeability and is easily contaminated when processing aqueous solutions containing several natural organic and colloid materials, which are susceptible to deposition and absorption into the membrane surface (Brites Alves et al., 2002). Therefore, much of the research on PVDF membranes has focused on increasing hydrophilicity through various methods, including improving membrane separation processes and modification of existing membrane surfaces (Cao, 2014).

2. Membrane PVDF

The membrane of polyvinylidene fluoride (PVDF) is a pure thermoplastic fluorine polymer formed by vinylidene difluoride polymerization with the chemical formula C2H2F2. Due to its excellent anti-oxidation activity, PVDF is one of the most widely used membrane materials in recent times for oil separation from oily wastewater, Highly organic selectivity, strong mechanical forming strength that enables re-examination and storage, excellent processing facilities (Masuelli, 2013), ease of control of structural and morphological characteristics, excellent aging resistance, high binding power, excellent chemical resistance and thermal stability, large processing temperature and ductility shown in Table 1. In contrast to other organic polymers such as PSF, PES, PVDF is relatively more hydrophobic, which may not be as high as polypropylene (PP) and polytetra fluoroethylene (PTFE). Generally, the hydrophobicity of polymeric materials is generally associated with their critical surface tension. PVDF is readily soluble in common organic solvents such as N, N-dimethylacetamide (DMAc), N, N-dimethylformamide (DMF), N-methylpyrrolydone (NMP) and Acetone, and as a result, the porous PVDF membrane is readily formed via non-induced phase separation. solvent (NIPS). Apart from that, its excellent thermal stability, semi-crystalline properties have made PVDF an attractive membrane material. The ability to choose the right material for the formation of PVDF

membranes as well as the best membrane preparation techniques play a very important role in the performance of PVDF membranes.

Such factors, however, may not be sufficient to achieve top results. Phase inversion, interface polymerization, electro spinning, stretching, and traverse etching are the most widely used techniques for the preparation of PVDF membranes. The most widely used techniques for the manufacture of PVDF membranes are phase inversion, interface polymerization and electro-spinning, among the previously described techniques. A controlled transformation of a thermodynamically stable or homogeneous polymer solution from a liquid to a porous solid is involved in the phase inversion process. Non-solvent-induced phase separation (NIPS), thermally induced phase separation (TIPS), evaporation-induced phase separation (EIPS), and phase separation steam-induced (VIPS) can induce phase separation from the casting solution to the lean PVDF polymer and the rich phase of the PVDF polymer (Lalia et al., 2013).

Table 1. Characteristics of PVDF (Lovinger, 1981)

Character	Value
Form	White solid
Solubility	Non-soluble in water
Elongation	12 – 600%
tensile strength	21,0 – 57,0 MPa
modulus of elasticity	1380 – 55.200 MPa
Glass temperature transition (Tg)	-60 – -20^{o}C
Melting Temperature	141 – 178^{o}C

Although, these reasons may not be sufficient to achieve top performance. The most commonly used techniques for the preparation of PVDF membranes include phase inversion, interface polymerization, electro spinning, stretching, and traverse etching. Among the previously mentioned techniques, phase inversion, interface polymerization and electro-spinning are the most commonly used techniques for the manufacture of PVDF membranes. The phase inversion process involves a controlled transformation of a thermodynamically stable or homogeneous polymer solution from a liquid to a porous solid. The phase separation from the casting solution to the lean PVDF polymer and the rich phase of the PVDF polymer can be induced by: non-solvent-induced phase separation (NIPS), thermally induced phase separation (TIPS), evaporation-induced phase separation (EIPS) and phase separation steam-induced (VIPS) (Lalia et al., 2013).

3. Hydrophilic membrane and antifouling

The hydrophilic-hydrophobic design of the polymer material that makes up the membrane is one of the essential aspects in the process of membrane filtration. By looking at the angle of touch between the membrane surface and the liquid, this property can be determined. A broad contact angle of 90 ° or more is characterized by hydrophobic properties, whereas numbers below

90 ° are known as hydrophilic materials (Yuan, 2013). Polymeric materials are typically membranes with hydrophobic constituents such as PES, PSF, PAN and PVDF for processes that use pressure as a forced drive. This is because this polymer has very good mechanical, chemical and thermal properties, but due to strong adhesion-adsorption forces, it is very susceptible to fouling due to foulant interactions with the membrane surface, almost no hydrogen bonding interactions in the boundary layer between the membrane interface and water (Kochkodan & Hilal, 2015). The repulsion of water molecules moving away from the hydrophobic membrane surface is a random phenomenon that causes foulant molecules to begin to adsorb to the surface of the membrane and to control the boundary layer and the process of polarization of concentration that occurs during the process of filtration.

In comparison, high surface tension membranes with hydrophilic layers are capable of forming hydrogen bonds with adjacent water molecules for the reconstruction of the thin water boundary between the membrane and the condensed liquid. This layer will avoid or minimize contaminants attached to the surface of the membrane (Kochkodan & Hilal, 2015). In this case, the fouling-resistant membrane not only decreases protein adsorption greatly, but is also capable of preventing microbial adhesion.

4. PVDF membrane surface modification

There are many methods of modification to transform the properties of the membrane surface into antifouling by means of physical modification (coating, mixing and use of composite membranes) and chemical modification, according to (Ayyavoo et al., 2016) (polymer functionalization, plasma processing). And polymerization of the graft).

Three different mechanisms physically place hydrophilic functional materials on the membrane surface: (1) macroscopic binding of functional groups and membrane pore structures, (2) interpenetration through the interface combination of functional materials and simple polymers, and (3) adhesion/adsorption (Ayyavoo et al., 2016).

4.1.Surface coating

In the case of a surface coating, the membrane is soaked in a polymer-containing solution in order to enhance the properties of the current antifouling membrane (Lalia et al., 2013). Poly (vinyl alcohol) (PVA), chitosan and poly (block ether amide) (PEBAX) are hydrophilic polymers which are commonly used due to the poor physical adsorption interaction between PVDF membranes and layered layers for hydrophilic modification of PVDF membranes (Kang and Cao, 2014). During the operation, the latter appears to be lost. Surface grafting, on the other hand, may be applied to the membrane surface to overcome the instability issue of the coated layer. The surface modification path, including surface resurfacing and surface grafting, is shown in Figure 1. (Liu et al., 2011). Due to its high hydrophilicity, biocompatibility, mechanical strength and thermal stability, PVA can be used as a hydrophilic surface for membranes

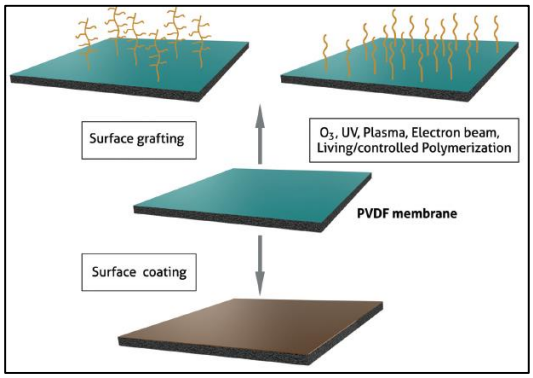

Figure 1. The route of surface modification, including surface coating and surface grafting (Abed K.Li, 2011).

In addition, improved biofouling resistance has been shown by PVA coated surfaces. The contact angle decreased from 81 ± 1 ° to 68 ± 1 ° after modification, with the addition of PVA (Du et al., 2009). The modified membrane displayed a greater flux and slower fouling rate relative to the unmodified membrane during natural water filtration. A double-layered PVDF hollow fiber membrane (HFM) was modified by coating it with dopamine and grafting polyethylene in a study conducted by Shi et al (2016). Through the quaternization reaction shown in Figure 2, researchers obtained hydrophilic and antibacterial membranes. The results obtained were the pure water flux value (PWF) before and after the bovine serum albumin contamination (BSA) measurement, and the rate of flux recovery. The changed membrane had reached 94.%.

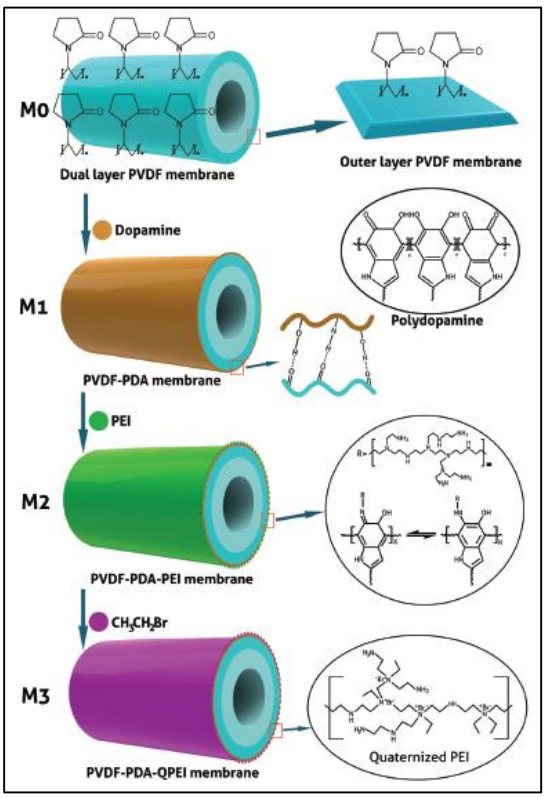

Figure 2. A hydrophilic and antibacterial membrane through quaternisation reactions (Shi et al,2016).

4.2.Surface grafting

Transplants are carried out by changing the membrane surface surface by covalent bonding interactions between hydrophilic compounds and membranes in the chemical chain. The covalent bond on the surface of the resulting membrane, unlike the surface layer, would have greater chemical stability than that of the surface layer. The technique of surface grafting, however, has a weakness, namely that the graft compound can block the membrane pores and reduce the performance of the membrane, namely the permeability and flux produced (Moghareh Abed et al., 2013). In several models, such as plasma treatment grafting, managed polymerization grafting and UV photography, the surface grafting process can be carried out. Rahimpoor with a scientific dip coating was an example of changing the PVDF membrane, followed by UV irradiation using benzophenone as a photoinitiator. In order to improve hydrophilicity, they used acrylic acid (AA) and 2-hydroxyethylmethacrylate (HEMA) as acrylic monomers and 2,4-phenylenediamine (PDA) and ethylene diamine (EDA) as amino monomers at different concentrations, thereby minimizing fouling tendencies. After alteration, the PVDF membrane's hydrophilicity, antifouling properties and flux recovery were all enhanced.

4.3. Plasma polymerization

The electrical ionization of the monomers is plasma polymerization, resulting in fragments of reactive monomers. The benefits of plasma polymers over traditional polymers are that this technique has a much higher degree of cross-linking and is tightly bound to the substrate, and the coating is uniform and does not require the use of harsh solvents that can damage the substrate (Zou et al., 2011).With rising surface PEG graft concentrations, the researchers found that PWF decreased, while the mean pore size remained almost unchanged. In addition, the experiments on protein adsorption and water flux showed that the PEG-g-PVDF membrane exhibited strong anti-fouling properties with a graft concentration ([CO] / [CF2]) above 3.2 as a simple dipping coating technique using inverted super-hydrophilic silica nanoparticles on a poly (methacrylic acid) copolymerized membrane surface (PMAA) (Liang et al., 2013) shown in Figure 3.

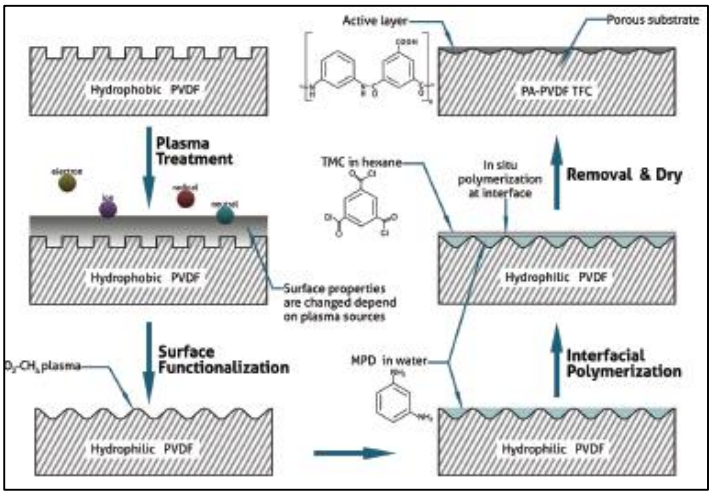

Figure 3. Using the post-fabrication method, super-hydrophilic silica nanoparticles are irreversibly bound to the poly(methacrylic acid) (PMAA) graft-copolymerised PVDF membrane surface using a simple dip-coating technique (Liang et al, 2013).

With this process, modification is capable of changing the properties of the PVDF membrane from hydrophobic to hydrophilic conditions and forming a layer of hydration on the -OH group. It also has excellent antifouling properties (Liang et al., 2013).

5. Conclusions

In the treatment of aqueous solutions containing some natural organic and colloid materials, which are susceptible to deposition and absorption to the membrane surface, the strong hydrophobic properties of pure PVDF membranes often lead to low water permeability and fast contamination. There are many methods of modification to alter the surface properties of the antifouling membrane by physical modification (coating, mixing and use of composite membranes) and chemical modification (polymer functionalization, plasma processing and graft polymerization). Several methods of increasing membrane hydrophilicity, such as surface coating, surface grafting, and plasma polymerization, will be addressed in this review article.

Reference

1. A.M.Brites Alvesa; A.Morão; J.P.Cardosob. (2002). Isolation of antibiotics from industrial fermentation broths using membrane technology. *Desalination*, *148*(1–3), 181–186.
2. Abed, M.R.Moghareh;Kumbharkar, S.C; Groth, A.M.;Lia, K. (2013). Economical production of PVDF-g-POEM for use as a blend in preparation of PVDF based hydrophilic hollow fibre membranes. *Separation and Purification Technology*, *106*, 47–55.
3. AbedK.Li, F. L. N. A. H. Y. L. M. R. M. A. K. L. (2011). Progress in the production and modification of PVDF membranes. *Journal of Membrane Science*, *375*(1–2), 1–27.
4. Ayyavoo, Jayalakshmi ; Nga Nguyen, Thi Phuong; Jun, Byung-Moon; Kim,In-Chul ; Kwon, Y.-N. (2016). Protection of polymeric membranes with antifouling surfacing via surface

modifications. *Colloids and Surfaces A: Physicochemical and Engineering Aspects*, *506*, 190–201.

5. Cao, G. K. Y. (2014). Application and modification of poly(vinylidene fluoride) (PVDF) membranes – A review. *Journal of Membrane Science*, *463*, 145–165.
6. Catherine Charcosset. (2009). Preparation of emulsions and particles by membrane emulsification for the food processing industry. *Journal of Food Engineering*, *92*(3), 241–249.
7. François Zaviska , Patrick Drogui, Alain Grasmick, Antonin Azais, M. H. (2013). Nanofiltration membrane bioreactor for removing pharmaceutical compounds. *Journal of Membrane Science*, *429*, 121–129.
8. Hilal, Nidal; Ogunbiyi, Oluwaseun O; Miles,Nick J; Nigmatullin, R. (2005). Methods Employed for Control of Fouling in MF and UF Membranes: A Comprehensive Review. *Separation Science and Technology*, *40*(10), 1957–2005.
9. Kang, G., & Cao, Y. (2014). *Application and modi fi cation of poly (vinylidene fl uoride) (PVDF) membranes – A review*. *463*, 145–165. https://doi.org/10.1016/j.memsci.2014.03.055
10. Khayet, M., & Matsuura, T. (2001). Preparation and Characterization of Polyvinylidene Fluoride Membranes for Membrane Distillation. *Ind. Eng. Chem. Res*, *40*, 5710–5718.
11. Kochkodan, V; Hilal, N. (2015). A comprehensive review on surface modified polymer membranes for biofouling mitigation. *Desalination*, *356*, 187–207.
12. Liang,Shuai;Kang,Yan;Tiraferri,Alberto;P. Giannelis,Emmanuel;Huang, Xia;Elimelech, M. (2013). Highly Hydrophilic Polyvinylidene Fluoride (PVDF) Ultrafiltration Membranes via Postfabrication Grafting of Surface-Tailored Silica Nanoparticles. *ACS Appl. Mater. Interfaces*, *5*(14), 6694–6703.
13. Lovinger, A. J. (1981). *Poly(vinylidene Fluoride)*. Bell Lab.
14. M. Elimelech, W.A.Phillip. (2011). The future of sea water desalination. *Energy, Technology, and the Environment Science*, *333*, 712–717.
15. Masuelli, A. . (2013). Synthesis polysulfone-acetylethanol ultrafiltration membranes. Application to oily wastewater treatment. *Journal of Materials Physics and Chemistry*, 37–44.
16. R.Du, Jennifer ; Peldszus, Sigrid;M.Huck, Peter ;Feng, X. (2009). Modification of poly(vinylidene fluoride) ultrafiltration membranes with poly(vinyl alcohol) for fouling control in drinking water treatment. *Water Research*, *43*(18), 4559–4568.
17. S. Liang, Y. Kang, A. Tiraferri, E.P. Giannelis, X. H. and M. E. (2013). ACS. *Applied Materials and Interfaces*, *5*, 6694–6703.
18. Shi, Huyan; Xue, Lixin;Gao, Ailin;Fu, Yinyi;Zhou, Qingbo;Zhu, L. (2016). Fouling-resistant and adhesion-resistant surface modification of dual layer PVDF hollow fiber membrane by dopamine and quaternary polyethyleneimine. *Journal of Membrane Science*, *498*, 39–47.
19. Singh Lalia, Boor; Kochkodan, Victor ; Hashaikeh, Raed; Hilal, N. (2013). A review on membrane fabrication: Structure, properties and performance relationship. *Desalination*, *326*, 77–95.
20. Y.Zhang, J.Sunarso, S.M.Liu, R.Wang, Y.Zhang, J.Sunarso, S.M.Liu, R. W. (2013). Current status and development of membranes for CO2/CH4 separation: a review. *Int.J.Greenh.GasControl*, *12*, 84–107.
21. Yuan,Y; Lee, T. R. (2013). Contact angle and wetting properties, Surface science techniques. *Springer*, 3–34.
22. Zou, L;Vidalis, I;Steelec, D; Michelmore, A;Low, S. P. J. Q. J. C. V. (2011). Surface hydrophilic modification of RO membranes by plasma polymerization for low organic fouling. *Journal of Membrane Science*, *369*(1–2), 420–428.

Journal of Membranes and Materials v(i) pp-pp (YYYY)
Received Month Year / Revised Month Year / Accepted Month Year

Journal of Membranes and Materials

https://ejournal2.undip.ac.id/index.php/jmm

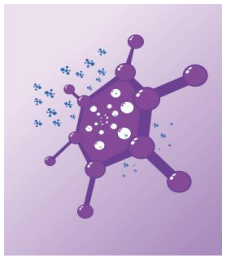

REVIEW ARTIKEL: TECHNOLOGY REVERSE ELECTRODIALYSIS MEMBRANE

Assalaam Umar Abdurahman[1)]

[1)]*Department of Chemical Engineering, Faculty of Engineering, Diponegoro University*
No. 1 Prof. H. Soedarto, SH Road, Tembalang-Semarang, INDONESIA 50275
Tel. (62)-24-7460058; Fax: (62)-24-76480675
**e-mail: assalam0904@gmail.com*

Abstract. *The level of world energy consumption is increasing continuously, so that environmental impacts such as CO_2 emissions are increasing. The renewable energy source that has great potential in the world is the Salinity Gradient Power, which utilizes energy from mixing sea water and river water. Reverse Electrodialysis is one of the most promising methods to capture salinity gradient power to solve energy demands in the future due to being environmentally-friendly in producing no emission pollutant gases and producing a high density of energy, which generates power via the transport of the positive and negative ions in the water through selective ion-exchange membranes.Ion-exchange membranes are used in environmental and energy technologies of electrodialysis desalination and reverse electrodialysis power generation, respectively. Recent studies reported empirical evidence that the conductivity and permselectivity of IEMs are bound by a tradeoff relationship, where an increase in ionic conductivity is accompanied by a decrease in counterion selectivity over co-ion. The analysis revealed the mechanism for the tradeoff induced by bulk solution concentration: a higher salinity suppresses IEM charge-exclusion, thus lowering permselectivity, but elevates mobile ion concentration within the membrane matrix to improve conductivity. As such, IEM applications are practically confined to sub-seawater salinities, i.e., RED using hypersaline streams will not be efficient. In another tradeoff driven by IEM water sorption, increasing membrane swelling enhances effective on diffusivity to raise conductivity, but diminishes permselectivity due to dilution of fixed charges.*

Keyword : *CO_2, IEM, reverse electrodialysis, salinity*

1. Introduction

The development of renewable and environmentally friendly energy is very important in reducing dependence on the use of fossil fuels. This is because the level of world energy consumption increases continuously, so that environmental impacts such as CO_2 emissions are increasing [1-4,14-17]. Salinity Gradient Power is a renewable energy source with great potential in the world, namely utilizing energy from mixing seawater and river water. Approximately 0.70-0.75 kWh of energy is released when 1 m^3 of river water mixes with 1 m^3 of seawater. SGP is a promising renewable energy that does not cause emissions so that it can be categorized as clean energy [9-11,22-25]. The two most promising methods of applying Salinity Gradient Power are Pressured Retarded Osmosis and Reverse Electrodialysis. The Reverse

Electrodialysis method generates electrical energy using ion flow which is induced when salt water and fresh water are mixed through Ion Exchange Membranes. One of the important factors to increase the efficiency of the Reverse Electrodialysis process is the improvement of the transport properties of the Cation Exchange Membrane [12].

The development of a Cation Exchange Membrane with special characteristics, such as selectivity, ionic conductivity, permeability and high chemical, thermal and mechanical resistance is desirable. So it must be considered in the selection of ion exchange membranes that have long lasting properties chemically and mechanically [15]. investigated the preparation of Cation Exchange Membrans magnetic matrices by inserting cobalt ferrite nanoparticles into a PVC membrane [4,6]. The addition of $CoFe_2O_4$ nanoparticles in the membrane matrix caused an increase in membrane conductivity and surface hydrophility, but the addition of $CoFe_2O_4$ that was too high caused a decrease in the permeability and properties of the membrane [5,6].

GO has a specific surface area and high mechanical strength, flexibility, and atomic level thickness so that the addition of GO to polymer membranes can improve membrane performance, such as hydrophility, conductivity, and membrane permeability [32-35]. Unused battery waste can be utilized graphite rods for membrane additives. Renewable energy sources have received significant attention due to limited fossil fuel sources and global warming . The oceans represent a vast and largely untapped source of energy [31].

One of the forms is the salinity gradients. RED is one of the most promising methods to capture salinity gradient power to solve energy demands in the future due to being environmentally-friendly in producing no emission pollutant gases and producing a high density of energy , which generates power via the transport of the positive and negative ions in the water through selective ion-exchange membranes [30,42-44] . Ion-exchange membranes are charged polymeric films that allow the selective transport of oppositely-charged species , while retaining the like-charged ions and water . IEMs are employed in environmental and energy technologies, such as desalination, fuel cells, and salinity gradient power generation , and also chemical production by the chloralkali process [45] .

Reverse electrodialysis , the power generation analog of ED, converts the chemical potential energy stored in salinity gradients to useful electrical work by the directional permeation of ions across the charge-selective membranes [49] . Demonstrated that the use of hot and highly concentrated brine discharged from MD could improve the RED efficiency by increasing the salinity gradient and decreasing the electrical resistance. One important factor for increasing the efficiencies of the mentioned processes is improvement in transport properties of cation exchange membranes such as ion exchange capacity, ionic conductivity and permselectivity [47,50]. Selecting chemically and mechanically durable ion exchange membranes for applying in their harsh environments is necessary. Polyvinyl chloride is one of the most extensive thermoplastic materials in the world due to its valuable properties, wide applications, high chemical resistance, barrier properties and low cost [2,4,6] . However, PVC has a low ion exchange and conductivity.

This study analyzes ion transport across IEMs to elucidate the dependence of key performance parameters, ionic conductivity and charge selectivity, on intrinsic membrane chemical and structural properties. Firstly, the working principles of ion-exchange membranes, electrodialysis, and reverse electrodialysis are described. The underpinning phenomena relating operating conditions and membrane properties to IEMs performance are highlighted and the principal factors governing the observed

conductivity-permselectivity tradeoff are elucidated [32]. Lastly, the implications for ED desalination, RED salinity gradient power generation, and membrane development are discussed.

2. Principles of ion-exchange membranes and IEM processes

2.1. Electrochemical membrane processes

Fig. 1 provides a useful overview of the relationship between electrodialysis (ED), RED, short-circuit reverse electrodialysis (SRED), voltage assisted reverse electrodialysis (VARED), and diffusion dialysis (DD). ED is a well-established desalination method, where an external electrical voltage is applied to overcome the electromotive force (in addition to any overpotential at the electrodes) such that ions migrate against their respective concentration gradient to obtain desalted water. In contrast, the electrical voltage in RED is lower than the electromotive force such that ions move under the concentration gradient to generate an ionic current that has opposite direction to the electrical field. Whereas ED consumes electricity, its reverse process RED produces electricity from salinity gradient; their power density is given by the product of the electrical voltage output and the corresponding current density. Under the special condition where the electrical voltage output is 0 (close-circuit condition), electricity is neither produced nor consumed. In this case, ions can diffuse under their respective concentration gradients at rates faster than the corresponding ones under RED conditions; this process is referred as SRED in this paper. To further enhance the rates of transport of ions, an external voltage can be applied in the same direction to the ionic current. This configuration, referred as VARED, accelerates the ion removal from the high concentration stream at the expense of additional energy consumption compared to SRED. Both SRED and VARED can have potential applications in desalination by removing salts from the high concentration solution at accelerated rates.

The electrochemical membrane processes ED, RED, SRED, and VARED are analogous to their pressure/ osmotic-pressure-driven counterparts reverse osmosis, pressure retarded osmosis, forward osmosis, and pressure-assisted forward osmosis, respectively [35]. DD is a process similar to SRED in that no external voltage is applied. However, instead of using both AEMs and CEMs in an alternative sequence in SRED, only one type of membrane is used in DD. DD processes using AEMs are commonly applied for recovering acids [30–34]. In these applications, the transport of anions (e.g., Cl^-, SO_4^{2-} or NO_3^-) under their concentration gradient across an AEM is accompanied by H+ as a counter-ion due to its small size and high mobility; electroneutrality is maintained during the transport of ions such as no net electric current is produced [45]. For this reason, DD is located at the origin of the plot in Fig. 1a,b. In a similar manner, DD processes using CEMs can be used for separating base containing solutions [45]. To further accelerate the ions migration in DD, a voltage assisted diffusion dialysis (VADD) can be used by applying an external electric field in the same direction as the concentration gradient [46].

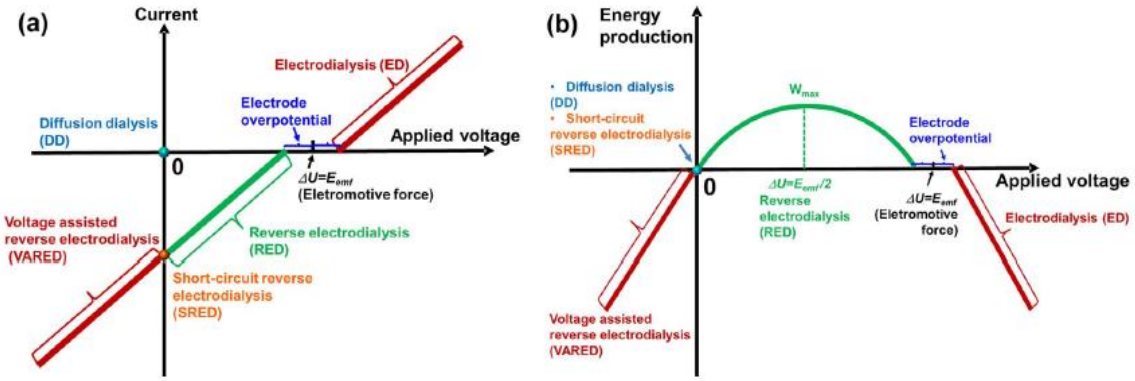

Fig. 1. (a) Current as a function of applied voltage in ED, RED, SRED, VARED, and DD; (b) energy output as a function of applied voltage in ED, RED, SRED, VARED, and DD. ED process where electrical energy is consumed to drive ionic transport against the concentration gradient; RED process where electricity is generated from ionic current along the concentration gradient; VARED process where electricity is consumed to further enhance the ionic transport from the concentrated solution to dilute solution; SRED and DD processes where electricity is neither consumed nor generated.[28]

2.2. Working principles of ion-exchange membranes

Ion-exchange membranes are water-swollen polymeric films of typically 50-200 m thickness, with a high density of charged ionic functional groups fixed to the backbone chains [1, 30, 31]. The selective transport of IEMs is achieved by the charge exclusion principle: the fixed functional groups exclude like-charged co-ions and the membrane preserves electroneutrality by having a high concentration of counterions (opposite charge to fixed moieties). Ion transport is driven by electrochemical potential, and the comparatively greater concentration results in a larger flux of counterions than co-ions. Hence, IEMs allow the preferential permeation of counterions over co-ions, but because co-ions are not completely excluded from the membrane matrix, the charge selectivity of IEMs is imperfect. Cation exchange membranes (CEMs) with fixed negatively charged functional groups, such as, sulfonic acid, phosphoric acid, and derivatives of sulfonamide and azole, selectively favor cations permeation; whereas anion exchange membranes (AEMs) possess cationic functional groups, e.g., quaternary ammonium, to
facilitate transport of anions over cations [32, 33].

2.3. Electrodialysis desalination

Electrodialysis (ED) is an IEM-based desalination technology that utilizes an electric current to separate charged ions from a saline stream and produce freshwater [2, 7]. In ED, an external electric potential is applied across a stack comprising repeating pairs of CEM and AEM. Saline feed stream flows through each compartment channel between the membranes. The external electric potential drives the permeation of cations towards the cathode and the anions towards the anode. As the IEMs selectively allow the permeation of counterions and retain co-ions, cations and anions permeate into the concentrate compartment from the abutting diluate streams, across the CEM and AEM, respectively, but ions in the concentrate stream are hindered from crossing into the diluate compartment (Fig. 2).

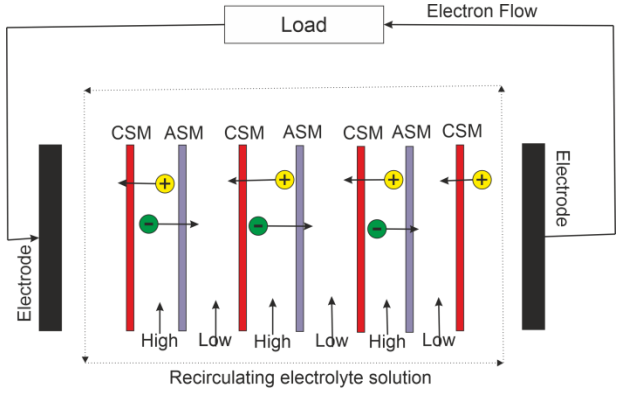

Fig 2. Reverse Electrodialysis (RED) - CEM: cation exchange membrane; AEM: anion exchange membrane.

2.4. Reverse electrodialysis energy production

Reverse electrodialysis (RED) produces useful work from salinity gradients by inverting the operating principles of ED separation [9, 34]. Instead of supplying external electrical energy, RED generates power

from the controlled mixing of high and low concentration solutions. A similar membrane stack configuration as ED is utilized: a repeating cell consists of, in spatial order, a CEM, a high concentration (HC) solution compartment, an AEM, and a low concentration (LC) solution compartment (which is bordered by the CEM of the next cell). This alternating structure enables the series addition of Nernst potentials arising from the concentration difference across the IEMs. Selective transport of anions and cations in the HC solution, across the AEM and CEM, respectively, to the adjacent LC chambers produces a net charged ion flux. Like ED, a reversible redox couple is circulated between the two end electrode chambers to transform ionic current in the stack to an electric current that powers the load in the external circuit.

2.5. Ion exchange capacity

The ion exchange capacity (IEC) of cation exchange membranes was measured by acid-base titration method. Membrane samples were immersed into excess 1 M HCl solution for 24 hours to saturate all the fixed charged groups with H+; then the samples were washed with demi-water until the surface water was completely removed. Following this, the samples were immersed into 40 ml of 2 M NaCl solution to exchange H+ with Na+ and to release H+ into solution. This step was repeated 3 times for a complete exchange. Finally, the immersed solutions were collected into a beaker and titrated with 0.01 M NaOH. The titration was continued until the pH of the collected solution reached the pH of the initial 2 M NaCl solution [35]. The pH values were monitored with a pH meter (WTW Inolab Terminal Level 3, Germany).

2.6. IEC (Ion Exchange Capacity) Analysis

The cation exchange membrane was immersed in 1M HCl for 15 hours, and then immersed using deionized water for 1 hour to be free from chloride. Then the membrane was immersed in 1 M NaCl solution for 6 hours. The hydrogen ions removed from the membrane were then titrated with 0.01 M NaOH solution and used the phenolphtalein indicator. The IEC is calculated using the following equation [19]:

$$IEC = \frac{Cx\,V}{W}$$

with:
IEC = ion exchange capacity (meq / g)
C = molar concentration of the titrant (M)
V = volume of titrant (ml)
W = dry membrane sample weight (grams)

2.7 Porosity

The porosity test was carried out to determine the amount of membrane porosity [52]. The pore structure affects the ion conductivity. Porosity was measured by weighing the dry weight of the membrane, then immersing the membrane in demin water for 24 hours. Then weigh the membrane wet weight. The porosity can be calculate with equation [51]:

$$Porosity = \frac{m_{wet}x\,m_{dry}}{AL\rho_w}$$

with:
m_{wet} = wet weight (g)
m_{dry} = dry weight (g)
A = membrane area (cm)

L = membrane thickness (cm)
ρ_w = density of water (gram / ml)

3. Performance parameters for ED and RED

3.1. Current efficiency

Current efficiency, CE, is a measure of ionic current utilization in ED and RED for separation and energy production, respectively:

$$CE_{ED} = \frac{z_{ct}J_{ct}}{z_{co}J_{co}+z_{ct}J_{ct}} \qquad (1)$$

$$CE_{RED} = \frac{z_{co}J_{co}+z_{ct}J_{ct}}{z_{ct}J_{ct}} \qquad (2)$$

where *z* is the ion valence, *J* is the ion flux, and subscripts ct and co denote counter- and co-ions, respectively. Note that *z* and *J* can be positive or negative, depending on charge and direction, and the product *zJ* gives the ionic current. In ED desalination, the electric current drives counterand co-ion fluxes. These two ion fluxes flow in opposite directions and are of different charge, with only the counterion flux performing the desired function of desalinating the saline feed, whereas co-ion flux is an unwanted leakage of ions to the diluate stream that actually compromise desalination performance[24,27,38]. Current efficiency for ED desalination is, thus, the ratio of the current due to counterion flux to the total ionic current, Eq. 1. Conversely, the aim of RED is to generate an ion flux that can then be used to drive an external circuit and, hence, CERED is defined differently from ED desalination. Because both fluxes are in the same direction the current from counterion flux is partly negated by co-ion flux. The RED current efficiency, Eq. 2, is the net ionic current divided by the current due to counterion flux. Note that equation for CERED is the reciprocal of CEED. Current efficiency of ED and RED is analogous to the Faradaic efficiency of electrochemical processes, which quantifies the percentage of charge utilized for the desired electrochemical reaction[12].

3.2. Permselectivity

Permselectivity describes the selectivity for counterion transport and is defined as the ionic current carried by counterion flux less the current from co-ion flux, normalized by the total ionic current [1, 31]:

$$\alpha = \frac{|z_{ct}J_{ct}|-|z_{co}J_{co}|}{\sum|z_iJ_i|} = t_{ct} - t_{co} \qquad (3)$$

Note that the sign conventions of *z* and *J* are neglected and only the magnitude of the ionic currents are used to calculate . Further, the fraction of total ionic current carried by species *i* is the transport number, *ti*, and, hence, permselectivity is also the counterion transport number less the co-ion transport number (Eq. 3) [1]. An IEM with perfect charge selectivity is only permeable to counterions but not co-ions and, therefore, permselectivity equals to one. Experimentally characterized measurements are commonly reported in literature, but those values are more accurately termed “apparent permselectivity”, and is the ratio of measured open-circuit voltage (OCV) to theoretical Nernst potential [1]. Because of the ease of experimental characterization (one electrochemical reading instead of tracking counter- and coion concentration changes), apparent permselectivity is often used as a proxy parameter to approximate the fraction of ionic current carried by counter- and co-ions during actual ED and RED operation even though

it deviates from the definition of Eq. 3. Comparison between apparent and real permselectivities are discussed later in Section 5.

3.3. Area specific resistance

Area specific resistance, ASR, is defined in Eq. 17 as the slope of Vm with respect to the net current density, i_{tot} F (z_{co} J_{co} $z_{ct}J_{ct}$), i.e., differential resistance:

$$ASR = \frac{d\Delta V^m}{di_{tot}} \qquad (4)$$

Because the contribution of IEM to total internal resistance is significant in ED and RED [17], the membrane ASR should be small to suppress undesired resistive losses. In IEM processes, steady state current-voltage response can be described by one of the three regimes: ohmic (or under-limiting), plateau (or limiting), and overlimiting [49]. The current analysis will focus on simulating ion-exchange membranes working within the ohmic regime, which is the common operating conditions for ED and RED. In this relatively low current regime, i.e., under-limiting the relation between current density and imposed voltage is linear; ion depletion in the concentration polarization boundary layer is not dominant and a limiting current is not reached (i.e., before plateau regime).

3.4. Conductivity

Conductivity is the reciprocal of resistivity, and describes the ability of the IEM to conduct ionic currents:

$$\sigma = ASC\ x\ l = \rho^{-1} \qquad (5)$$

where ASC is the area specific conductance of membrane, which is equal to the multiplicative inverse of ASR, and l is the ion-exchange membrane thickness. It is instructive to note that conductivity and resistivity are intensive properties, i.e., independent of membrane physical dimensions, whereas ASC and ASR are extensive properties. Introducing and ASC enables the relationship between conductivity and permselectivity to be examined in an analytical framework akin to permeability-selectivity of gas separation and salt-rejecting membranes [10, 11].

4. Conclusion

The power of the salinity gradient can be converted directly to electricity using RED technology. This review summarizes the RED system of processes and items used. Innovations in RED stack components and system design are important aspects to improve RED power output performance. To date, several low IEMs adapted to high resistance and high permselectivity have appeared suitable for RED applications.

REFERENCES

[1] H. Strathmann, Ion-exchange membrane separation processes, Elsevier, 2004.

[2] H. Strathmann, Electrodialysis, a mature technology with a multitude of new applications, Desalination, 264 (2010) 268-288.

[3] S. Bose, T. Kuila, T.X.H. Nguyen, N.H. Kim, K.-t. Lau, J.H. Lee, Polymer membranes for high temperature proton exchange membrane fuel cell: recent advances and challenges, Progress in Polymer Science, 36 (2011) 813-843.

[4] G. Merle, M. Wessling, K. Nijmeijer, Anion exchange membranes for alkaline fuel cells: A review, J Membrane Sci, 377 (2011) 1-35.
[5] P. Długołęcki, K. Nymeijer, S. Metz, M. Wessling, Current status of ion exchange membranes for power generation from salinity gradients, J Membrane Sci, 319 (2008) 214-222.
[6] H. Strathmann, A. Grabowski, G. Eigenberger, Ion-exchange membranes in the chemical process industry, Industrial & Engineering Chemistry Research, 52 (2013) 10364-10379.
[7] T.W. Xu, C.H. Huang, Electrodialysis-Based Separation Technologies: A Critical Review, Aiche J, 54 (2008) 3147-3159.
[8] J.W. Post, H.V. Hamelers, C.J. Buisman, Energy recovery from controlled mixing salt and fresh water with a reverse electrodialysis system, Environ Sci Technol, 42 (2008) 5785-5790.
[9] N.Y. Yip, D. Brogioli, H.V.M. Hamelers, K. Nijmeijer, Salinity Gradients for Sustainable Energy: Primer, Progress, and Prospects, Environ Sci Technol, 50 (2016) 12072-12094.
[10] H.B. Park, J. Kamcev, L.M. Robeson, M. Elimelech, B.D. Freeman, Maximizing the right stuff: The trade-off between membrane permeability and selectivity, Science, 356 (2017).
[11] B.D. Freeman, Basis of permeability/selectivity tradeoff relations in polymeric gas separation membranes, Macromolecules, 32 (1999) 375-380.
[12] G.M. Geise, H.B. Park, A.C. Sagle, B.D. Freeman, J.E. McGrath, Water permeability and water/salt selectivity tradeoff in polymers for desalination, J Membrane Sci, 369 (2011) 130-138.
[13] A. Mehta, A.L. Zydney, Permeability and selectivity analysis for ultrafiltration membranes, J Membrane Sci, 249 (2005) 245-249.
[14] N.Y. Yip, M. Elimelech, Performance Limiting Effects in Power Generation from Salinity Gradients by Pressure Retarded Osmosis, Environ Sci Technol, 45 (2011) 10273-10282.
[15] G.M. Geise, M.A. Hickner, B.E. Logan, Ionic resistance and permselectivity tradeoffs in anion exchange membranes, Acs Appl Mater Inter, 5 (2013) 10294-10301.
[16] E. Guler, R. Elizen, D.A. Vermaas, M. Saakes, K. Nijmeijer, Performance-determining membrane properties in reverse electrodialysis, J Membrane Sci, 446 (2013) 266-276.
[17] N.Y. Yip, D.A. Vermaas, K. Nijmeijer, M. Elimelech, Thermodynamic, Energy Efficiency, and Power Density Analysis of Reverse Electrodialysis Power Generation with Natural Salinity
Gradients, Environ Sci Technol, 48 (2014) 4925-4936.
[18] A.H. Galama, D.A. Vermaas, J. Veerman, M. Saakes, H.H.M. Rijnaarts, J.W. Post, K. Nijmeijer, Membrane resistance: The effect of salinity gradients over a cation exchange membrane, J Membrane Sci, 467 (2014) 279-291.
[19] N. Berezina, N. Kononenko, O. Dyomina, N. Gnusin, Characterization of ion-exchange membrane materials: properties vs structure, Advances in Colloid and Interface Science, 139 (2008) 3-28.
[20] J. Kamcev, R. Sujanani, E.S. Jang, N. Yan, N. Moe, D.R. Paul, B.D. Freeman, Salt concentration dependence of ionic conductivity in ion exchange membranes, J Membrane Sci, 547 (2018) 123-133.
[21] B.P. Zhang, J.G. Hong, S.H. Xie, S.M. Xia, Y.S. Chen, An integrative modeling and experimental study on the ionic resistance of ion-exchange membranes, J Membrane Sci, 524 (2017) 362-369.
[22] J. Kamcev, D.R. Paul, G.S. Manning, B.D. Freeman, Ion Diffusion Coefficients in Ion Exchange Membranes: Significance of Counterion Condensation, Macromolecules, 51 (2018) 5519-5529.
[23] L.M. Robeson, H.H. Hwu, J.E. McGrath, Upper bound relationship for proton exchange membranes: Empirical relationship and relevance of phase separated blends, J Membrane Sci, 302 (2007) 70-77.
[24] K. Kontturi, L. Murtomäki, J.A. Manzanares, Ionic Transport Processes: In Electrochemistry and Membrane Science, Oxford University Press, 2008.

[25] A. Campione, L. Gurreri, M. Ciofalo, G. Micale, A. Tamburini, A. Cipollina, Electrodialysis for water desalination: A critical assessment of recent developments on process fundamentals, models and applications, Desalination, (2018).
[26] M. Tedesco, H.V.M. Hamelers, P.M. Biesheuvel, Nernst-Planck transport theory for (reverse) electrodialysis: I. Effect of co-ion transport through the membranes, J Membrane Sci, 510 (2016) 370-381.
[27] A. Moya, A Nernst-Planck analysis on the contributions of the ionic transport in permeable ion-exchange membranes to the open circuit voltage and the membrane resistance in reverse electrodialysis stacks, Electrochimica Acta, 238 (2017) 134-141.
[28] J. Kamcev, M. Galizia, F.M. Benedetti, E.S. Jang, D.R. Paul, B.D. Freeman, G.S. Manning, Partitioning of mobile ions between ion exchange polymers and aqueous salt solutions: importance of counter-ion condensation, Phys Chem Chem Phys, 18 (2016) 6021-6031.
[29] J. Kamcev, D.R. Paul, G.S. Manning, B.D. Freeman, Predicting Salt Permeability Coefficients in Highly Swollen, Highly Charged Ion Exchange Membranes, Acs Appl Mater Inter, 9 (2017) 4044-4056.
[30] T. Xu, Ion exchange membranes: state of their development and perspective, J Membrane Sci, 263 (2005) 1-29.
[31] T. Sata, Ion exchange membranes: preparation, characterization, modification and application, Royal Society of chemistry, 2007.
[32] J.G. Hong, B.P. Zhang, S. Glabman, N. Uzal, X.M. Dou, H.G. Zhang, X.Z. Wei, Y.S. Chen, Potential ion exchange membranes and system performance in reverse electrodialysis for power generation: A review, J Membrane Sci, 486 (2015) 71-88.
[33] J. Ran, L. Wu, Y.B. He, Z.J. Yang, Y.M. Wang, C.X. Jiang, L. Ge, E. Bakangura, T.W. Xu, Ion exchange membranes: New developments and applications, J Membrane Sci, 522 (2017) 267-291.
[34] M. Turek, B. Bandura, Renewable energy by reverse electrodialysis, Desalination, 205 (2007) 67-74.
[35] A.J. Bard, L.R. Faulkner, J. Leddy, C.G. Zoski, Electrochemical methods: fundamentals and applications, wiley New York, 1980.
[36] H.B. Callen, Thermodynamics and an Introduction to Thermostatistics, Wiley, 1985.
[37] F.G. Donnan, Theorie der Membrangleichgewichte und Membranpotentiale bei Vorhandensein von nicht dialysierenden Elektrolyten. Ein Beitrag zur physikalisch-chemischen Physiologie, Berichte der Bunsengesellschaft für physikalische Chemie, 17 (1911) 572-581.
[38] A. Galama, J. Post, H. Hamelers, V. Nikonenko, P. Biesheuvel, On the origin of the membrane potential arising across densely charged ion exchange membranes: How well does the Teorell-Meyer-Sievers theory work?, Journal of Membrane Science and Research, 2 (2016) 128- 140.
[39] G.S. Manning, Limiting laws and counterion condensation in polyelectrolyte solutions II. Self-diffusion of the small ions, The Journal of Chemical Physics, 51 (1969) 934-938.
[40] J. Kamcev, D.R. Paul, B.D. Freeman, Effect of fixed charge group concentration on equilibrium ion sorption in ion exchange membranes, Journal of Materials Chemistry A, 5 (2017) 4638-4650.
[41] R.A. Robinson, R.H. Stokes, Electrolyte Solutions ... Second edition, Butterworths Scientific Publications, London, 1959.
[42] K.S. Pitzer, Thermodynamics of electrolytes. I. Theoretical basis and general equations, The Journal of Physical Chemistry, 77 (1973) 268-277.
[43] K.S. Pitzer, G. Mayorga, Thermodynamics of electrolytes. II. Activity and osmotic coefficients for strong electrolytes with one or both ions univalent, The Journal of Physical Chemistry, 77 (1973) 2300-2308.
[44] F.G. Helfferich, Ion exchange, Courier Corporation, 1962.

[45] J.S. Mackie, P. Meares, The Diffusion of Electrolytes in a Cation-Exchange Resin Membrane .1. Theoretical, Proc R Soc Lon Ser-A, 232 (1955) 498-509.
[46] J.S. Mackie, P. Meares, The Diffusion of Electrolytes in a Cation-Exchange Resin Membrane .2. Experimental, Proc R Soc Lon Ser-A, 232 (1955) 510-518.
[47] J.G. Wijmans, R.W. Baker, The solution-diffusion model: a review, J Membrane Sci, 107 (1995) 1-21.
[48] D.R. Paul, Reformulation of the solution-diffusion theory of reverse osmosis, J Membrane Sci, 241 (2004) 371-386.
[49] N. Rosenberg, C. Tirrell, Limiting currents in membrane cells, Industrial & Engineering Chemistry, 49 (1957) 780-784.
[50] R. B.V, Dutch king officially opens Blue Energy pilot installation on the Afsluitdijk, http://www.redstack.nl/en/news/83/dutch-king-officially-opens-blue-energypilot-installation-on-the-afsluitdijk (November, 2014).
[51] Arsalan, M., Khan, M.M.A. & Rafiuddin. (2013). A comparative study of theoretical, electrochemical and ionic transport through PVC based Cu3(PO4)2 and polystyrene supported Ni3(PO4)2 composite ion exchange porous membranes. *Desalination. 318, 97–106.*
[52] Arifin, D. E. S., & Zainuri, M. (2014). Karakterisasi Sifat Separator Komposit PVDF / Poli (Dimetilsiloksan) dengan Metode Pencampuran Membran (*Blending Membrane)*. *Jurnal Sains & Seni Pomits, Vol. 3 No. 2, 2337-3520.*

Journal of Membranes and Materials v(i) pp-pp (YYYY)
Received Month Year / Revised Month Year / Accepted Month Year

Journal of Membranes and Materials

https://ejournal2.undip.ac.id/index.php/jmm

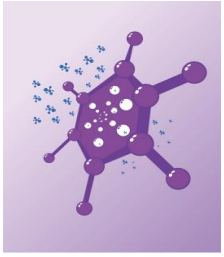

The Effect of Montmorillonite Concentration on Methanol Permeability and Methanol Uptake of Chitosan/Polivinil Alcohol-Montmorillonite Blend Membranes for Direct Methanol Fuel Cell Application

Shalahudin Nur Ayyubi[1*], Yunita Fahni [1,2], Lukman Atmaja[3]

[1]*Department of Chemical Engineering, Faculty of Engineering, Diponegoro University, Jl. Prof. Soedarto, Tembalang, Semarang 50275, Indonesia*
[2]*Membrane Research Center, Integrated Laboratory for Research and Services, Diponegoro University, Jl. Prof. Soedarto, Tembalang Semarang 50275, Indonesia*
[3]*Department of Chemistry, Faculty of Science and Data Analytics, Sepuluh November Institute of Technology, Surabaya, 60111, Indonesia*

Abstract. The synthesis of the chitosan / polyvinyl alcohol-montmorillonite (Cs / PVA-MMT) composite membrane was carried out using the phase inversion method. The effect of concentration MMT on the absorption and permeability of the membrane was investigated. The FTIR results showed that the CS / PVA-MMT composite membrane was successfully synthesized. Modification of chitosan with polyvinyl alcohol (3: 1) (w / w) improved the properties and performance of composites. Montmorillonite with a concentration of 2% shows the best results, with the percentage value of methanol absorption of 29.76%, water absorption of 46.93%, and permeability of methanol of 1.433 x 10^{-7} cm^2 s^{-1}.
Keywords: Chitosan; Composite Membrane; Direct Methanol Fuel Cell; Montmorillonite; Polyvinyl Alcohol

1. Introduction

Polymer Electrolyte Membrane is an important component in DMFC, which functions as a proton conductor and separator of methanol between the cathode and the anode. Currently, such perfluorosulfonic acid membranes Nafion® is the primary membrane which is often used in the DMFC. Even though Nafion® has high conductivity proton, Nafion does not meet the requirements for low methanol permeability, especially at low temperatures (<100 °C). Hence the methanol permeation reduces the open-circuit voltage in its electrochemical cell system and contaminates the electrocatalytic process at the cathode (Cui et al., 2009).
Hydrophilic membranes such as chitosan (Cs) are widely used in membrane-based applications due to their high hydrophilic properties, good chemical properties, and thermal resistance properties. Because it has hydroxyl and amino groups, chitosan can chemically modify into various forms and can react in various chemical reactions that produce salt formation. Hydrophilic groups play a role important in water diffusion through the chitosan membrane. Chitosan is generally mixed with hydrophilic polymers to overcome the reduced mechanical

* Corresponding author's email: shalahudinnurayyubi@gmail.com, Tel.: +62-856-46333640;
doi: 10.14716/ijtech.v0i0.0000

strength in wet conditions. For example, polyvinyl alcohol (PVA) is a strong hydrophilic polymer and will quite well spread in the chitosan matrix when processed into it (Smitha et al., 2006). The blending of chitosan with PVA in the study previously can improve mechanical stability, methanol permeability, and proton conductivity (Yang & Chiu, 2012)

Montmorillonite (MMT), a type of clay smectite naturally available in abundance and free poison properties, is a promising ingredient in the mixture of various industries of food, medicine, cosmetics, and health. With the addition of MMT, thermal stability and the mechanical properties of bionanocomposites can be improved. However, when the clay content is high, it presents a strong tendency to clot. Therefore many experiments such as ultrasonic and organic irradiation have been was performed to disperse MMT (Guo et al., 2013).

In this study, chitosan will be modified using PVA with a concentration ratio of 3: 1, further doped with Montmorilont filler with various concentrations of 2, 4, 6, and 8% of the weight of chitosan. The purpose of this filler weight percent variation is to strengthen the interactions that occur between chitosan and montmorillonite. Hydrophobic properties owned by this montmorillonite, when used as a filler in the Cs / PVA composite membrane, will create new characteristics in these membranes' properties. Hence, this research carried out the manufacture of a composite membrane derived from chitosan, which acts as a polymer matrix organic and montmorillonite as inorganic fillers. This composite membrane was tested for methanol and water absorption, functional analysis groups, and methanol permeability as the inner membrane of the DMFC to determine its effectiveness as a polyelectrolyte membrane at various concentrations of montmorillonite.

2. Experimental Methods

2.1. Materials

Aquades (SAP Chemicals), shrimp shells (Penaeus monodon), montmorillonite K-10 (Sigma-Aldrich), polyvinyl alcohol (Merck), NaOH pellets (Merck), sulfuric acid solutions (SAP chemicals Indonesia), and acetic acid solutions (SAP Chemicals Indonesia).

2.2. Methods

2.2.1. Extraction of Chitosan

First of all, prepare dry shrimp shell powder. The shrimp skin is separated from the meat and cleaned to remove any stuck dirt. The clean skin is then dried. After that, the dry skin is collected and ground to form a powder. Furthermore, the results of grinding shrimp shells are sieved with a 40 mesh sieve.

Deproteination, the results of the 40 mesh sieve of 200 grams were dissolved in 3.5% NaOH with a ratio of 1: 10 (w / v) of powder to 3.5% NaOH. The dissolved powder was stirred using a magnetic stirrer for 2 hours at a temperature of 65 °C. The results of this stirring will form sediment and filtrate. The filtrate is separated from the sediment by the decantation method. The precipitate is washed using aqua DM to neutral pH, then filtered with a cotton cloth and dried in an oven for 4 hours at 105 °C. The result of heating in an oven in the form of the dry precipitate is then tested using ninhydrin to ensure protein is not present. The deproteination percentage is calculated using equation (1) below.

$$\%\ \text{Deproteination} = 100\% - \left[\frac{\text{Final weight}}{\text{Initial weight}}\right] x100\% \qquad (1)$$

Demineralization, the result of deproteination in the form of dry precipitate mixed with 1 N HCl solution in a ratio of 1: 15 (w / v). The result of mixing the precipitate with 1N HCl solution was stirred using a magnetic stirrer at 800 rpm for 30 minutes. The effect of stirring in the form of a mixture is allowed to settle, and the precipitate is separated from the filtrate by the decantation method. The precipitate was washed with aqua DM to neutral pH, then filtered with

a cotton cloth and dried in an oven for 4 hours at 105 °C. The resulting dry precipitate was analyzed using FTIR spectroscopy to confirm that the IR wave peaks belonged to chitin. The demineralization percentage is calculated using equation 2 as follows.

$$\%\,\text{Demineralization} = 100\% - \left[\frac{\text{Final weight}}{\text{Initial weight}}\right] x100\% \quad (2)$$

Deacetylation, the result of demineralization in chitin, is mixed with 50% NaOH solution with a ratio of 1: 10 (w / v) while heated for 4 hours at 120 °C. The mixture residue in the form of a mixture is separated from the filtrate using a Buechner funnel. Then, the precipitate obtained from the filter was washed with aqua DM to neutral pH and dried in an oven at 100 °C for 4 hours. The result of drying the chitosan precipitate was analyzed by FTIR spectroscopy to determine the degree of deacetylation and the suitability of the IR wave of chitosan with the standard. The percentage of deacetylation is calculated using equation 3 as follows. The final result of chitosan powder is shown in figure 1.

$$\%\,\text{Deacetylation} = 100\% - \left[\frac{\text{Final weight}}{\text{Initial weight}}\right] x100\% \quad (3)$$

Figure 1 Chitosan results of the chitin deacetylation process

2.2.2. Preparation of pure chitosan membrane

A total of 2 g of chitosan was mixed into 75 mL of 2% acetic acid then stirred and heated at 80 °C for 2 hours until homogeneous. The chitosan solution was put into the ultrasonic cleaner for 30 minutes. The solution is poured into an acrylic dish that has been rinsed with acetic acid and allowed to dry below room temperature to form a membrane sheet. The dried membrane was soaked with 1 N NaOH solution and washed with aqua DM to neutral pH. The membrane is allowed to dry below room temperature.

2.2.3. Preparation of Cs/PVA membrane

A total of 0.5 g of PVA was mixed into 12.5 mL aqua DM. Then stirred and heated to 70 °C for 2 hours until homogeneous, covered with plastic wrap. A total of 1.5 g of chitosan was mixed into 37.5 mL of 2% acetic acid solution. Then stirred and heated to 70 °C for 2 hours until homogeneous. The chitosan solution was put into the ultrasonic cleaner for 30 minutes. The two PVA solutions and chitosan solutions were mixed while stirring for 3 hours at room temperature until homogeneous. Then the solution was poured into an acrylic dish that had been rinsed with acetic acid and allowed to dry below room temperature to form a membrane sheet. The dried membrane was soaked with 2M H_2SO_4 solution and washed with aqua DM until a neutral pH. The membrane is allowed to dry below room temperature.

2.2.4. Preparation of Cs/PVA/MMT membrane

A total of 0.5 g of PVA was mixed into 12.5 mL aqua DM then stirred and heated to 70 °C for 2 hours until homogeneous in a closed state with plastic wrap. A total of 1.5 g of chitosan was mixed into 37.5 mL of 2% acetic acid solution, then stirred and heated to 70 °C for 2 hours until homogeneous. The chitosan solution was then put into the ultrasonic cleaner for 30 minutes. A total of 0.04 g; 0.08 g; 0.12 g; 0.16 g montmorillonite each dissolved in 25 mL of 2% acetic acid

until homogeneous. This solution is called the MMT solution. Furthermore, both PVA solutions and chitosan solutions were mixed while stirring for 3 hours at room temperature until homogeneous. This solution is called the Cs / PVA solution. The Cs / PVA solution is mixed with MMT solution while stirring and heated to 80 °C for 30 minutes, then put into an ultrasonic container for 30 minutes. The solution is then poured into an acrylic dish that has been rinsed with acetic acid and allowed to dry below room temperature to form a membrane sheet. The dried membrane was soaked with 2 M H_2SO_4 solution and washed with aqua DM until a neutral pH. The membrane is allowed to dry below room temperature. All the final results of the membrane that have been synthesized are shown in figure 2.

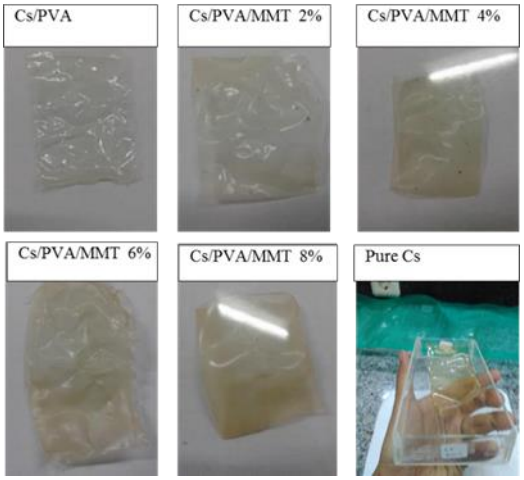

Figure 2 All membrane composites prepared by casting

2.2.5. FTIR analysis

The membrane to be analyzed for functional groups is taken with a thickness of 10 - 15 µm, then an analysis of measurements is carried out at a wavelength between 4000 - 400 cm^{-1} (Lavorgna et al., 2010).

2.2.6. Water uptake and methanol uptake measurements

The water uptake and methanol uptake tests were carried out by measuring the difference in membrane weight before and after immersion in water or methanol. Wet weight (W_{wet}) is measured from membranes immersed in 5 M water or methanol, while dry weight (W_{dry}) is measured from dried membranes for 24 hours at room temperature. For the calculation of water uptake and methanol uptake, the following equation is used.

$$\%\,\mathrm{WU} = \frac{W_{wet} - W_{dry}}{W_{dry}} \qquad (1)$$

2.2.7. Methanol permeability test

Compartments A and B are filled with methanol and distilled water, respectively, as shown in Figure 3, then a circular sample is placed between them (Wu et al., 2007). In the next testing process, each compartment containing methanol and distilled water was stirred. To test the permeability of methanol, a 5 M methanol solution will be used. Every 20, 40, 60, 80, 100 minutes, the compartment containing distilled water is taken as much as the pycnometer volume to determine the methanol concentration through a technique using a pycnometer. The permeability value of methanol is obtained using the equation (Yang & Chiu, 2012):

$$\%\,\mathrm{Permeability} = \frac{SV_B L}{AC_{A0}} xC_{A0} \qquad (1)$$

S is the slope of the chart; V_B (mL) is the volume of compartment B (distilled water); C_{A0} (mol

/ L) is the initial concentration of methanol in compartment A (methanol), L (cm) is the thickness of the membrane, and A (cm^2) is the area of the membrane.

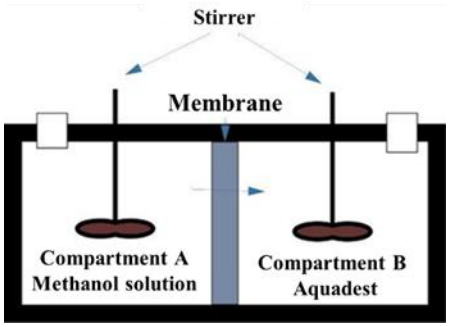

Figure 3 Illustration of methanol permeability test scheme (Neburchilov et al., 2007)

3. Results and Discussion

3.1. Fourier transformation infrared (FT-IR) spectra

To ensure the purity of chitosan, several qualitative and quantitative test parameters are necessary. The qualitative test can be seen from the absorption of functional groups from the FTIR spectra of chitosan; this distinguishes the shift in wavenumbers between chitin and chitosan. Meanwhile, the quantitative test is determined by calculating the degree of deacetylation (DD) of the transformation of chitin and chitosan. Figure 4 shows the results of FTIR characterization between chitin and chitosan. Generally, the absorption of infrared functional groups on chitosan can be seen in Table 1.

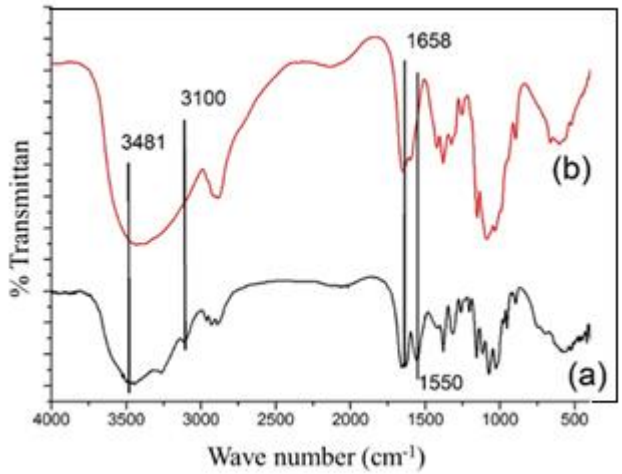

Figure 4 Comparison between FTIR between Chitin (a) and Chitosan (b)

Table 1 Types of functional group vibrations in chitosan

Wavenumber (cm^{-1})	Types of vibration	Vibration of functional group
3000 - 3500	Stretch	O-H and N-H
2926	Stretch	CH, CH3
1621	Stretch	C=O amide
1403	Buckling	C-H
1159	Stretch	C-O-C

Khan et al. (2012)

The success of the formation of this amine group (chitosan) can be determined quantitatively. Quantitative determination is done by calculating the deacetylation degree of chitosan. According

to (Khan et al., 2002), the degree of deacetylation of chitosan produced affects the quality and application of chitosan in various fields. Then the final result was chitosan with a deacetylation degree of 74.45%.

The FTIR test aims to see and confirm the formation of the Cs / PVA-MMT composite membrane that has been synthesized based on changes in functional groups. Figure 5 below presents the FTIR spectra of chitosan (CS) and CS/PVA / MMT membranes with montmorillonite concentrations of 2 and 8%.

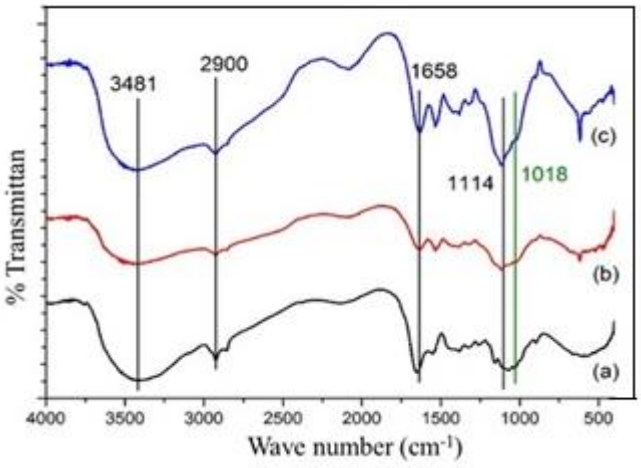

Figure 5 FTIR absorption results for Pure Cs (a), Cs/ PVA/MMT 2% (b), and Cs / PVA-MMT 8% (c) membranes

From the data obtained above, it shows that the CS / PVA / MMT composite membrane has been successfully synthesized, seen from the absorption of the functional groups formed, which is a combination of the spectrum of the constituent elements of the membrane, namely chitosan, polyvinyl alcohol, and montmorillonite. From Figure 5, it can also be estimated the effect of montmorillonite concentration on the CS / PVA / MMT membrane can be proven by the FTIR absorption, which is getting sharper along with the increasing concentration of montmorillonite in the 1108 cm^{-1} wavelength region, namely vibration of functional groups -Si- O and 618 cm^{-1} Al-O-Si vibration.

3.2. Water Uptake dan Methanol Uptake

To determine the membrane's ability to absorb water or methanol, a water uptake and methanol uptake test was carried out. This is done because the storage of water or methanol will determine the proton conductivity and membrane performance. The higher the water uptake value, the better the proton conductivity in the membrane; conversely, the higher the methanol uptake value, the worse the membrane performance is because too much methanol is absorbed, causing cross-over in the fuel cell, resulting in a decrease in voltage on the fuel cell. Figure 6 shows the water uptake and methanol uptake values of the composite membrane.

Based on the results obtained, overall, the Cs/PVA/MMT membrane that has been synthesized has a large water absorption capacity, which is around (40% -55%) and has a low methanol absorption, which is about (25% -35%) as shown in Figure 6. This is due to the nature of PVA, which is very hydrophilic and soluble in warm water but insoluble in alcohol solvents (Palani et al., 2014).

The graph also shows that the Cs / PVA membrane has a greater methanol absorption than the pure Cs membrane but has lower water absorption than pure Cs membranes. This is because the percentage of Cs is more dominant than PVA, which is 3: 1 w/w so that the membrane is semipolar and tends to absorb semipolar methanol more easily. On the other hand, the Cs / PVA membrane will decrease its ability to absorb water, which is more polar than methanol.

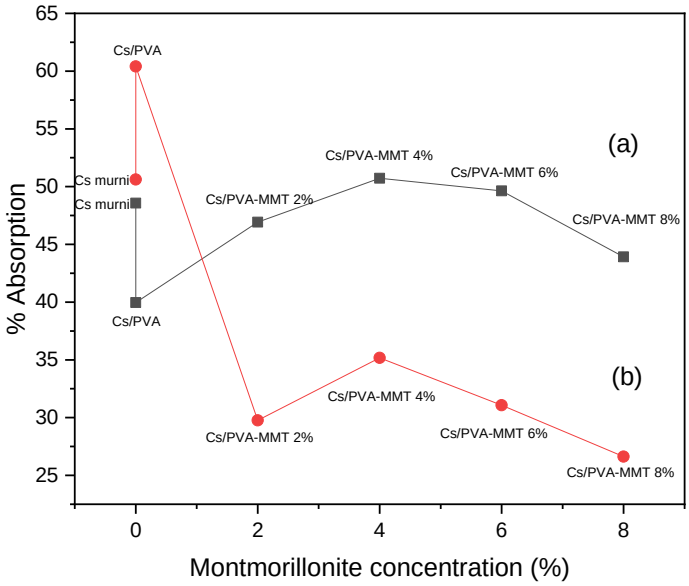

Figure 6 Results of the methanol uptake test (a) and water uptake (b)

Based on the graph, the addition of montmorillonite inorganic filler concentration tends to reduce the absorption of water and methanol (Umar et al., 2016). This phenomenon due to the nature of MMT's crystallinity and insoluble in chitosan solution. In this study, the membrane with the composition of Cs / PVA-MMT 2% had the best physical properties of all the synthesized membranes. Based on the graph, the addition of 2% MMT has a fairly large water absorption capacity and a small absorption capacity of methanol, which is proportional to the absorption capacity of water and methanol at the addition of 8% MMT.

3.3. Methanol permeability

To determine the membrane's performance for Direct Methanol Fuel Cell (DMFC) applications, a methanol permeability test was carried out. When the number of methanol molecules passing through the membrane is very large, it can cause a voltage drop, thus impairing the fuel cell's performance (Miyake et al., 2001).

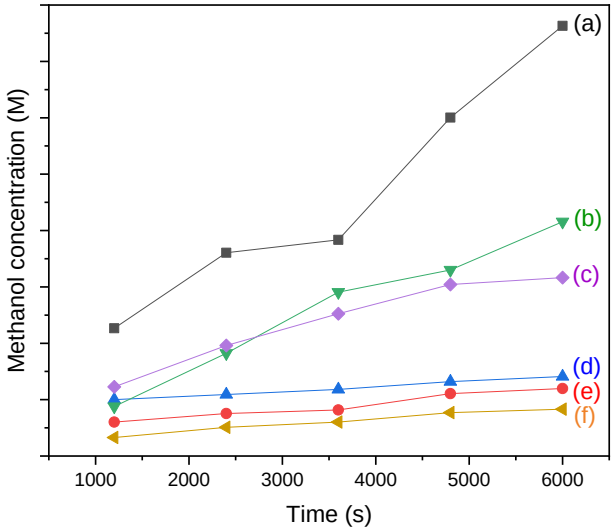

Figure 7 Graph of methanol concentration vs time (a) Pure Chitosan, (b) Cs / PVA-MMT 4%, (c) Cs / PVA MMT 6% (d) Cs / PVA-MMT 2% (e) Cs / PVA (f) Cs / PVA-MMT 8%

Based on figure 7, the permeability was determined by the slope of the relationship between time and concentration of methanol. After obtaining a membrane concentration curve for 5x20 minutes, the slope of the curve is used to calculate the permeability of methanol using the equation (5). Table 2 showed the results of the permeability of pure Cs, Cs / PVA, and Cs / PVA-MMT membrane methanol as follows.

Table 2 Methanol permeability of composite membranes

Membrane	Methanol permeability ($\times 10^{-7}$ cm^2 s^{-1})
Cs	31.84
Cs/PVA	3.98
Cs/PVA/MMT 2%	1.43
Cs/PVA/MMT 4%	22.29
Cs/PVA/MMT 6%	12.73
Cs/PVA/MMT 8%	2.38

Whereas Figure 8 shows the graph methanol permeability of composite membranes. Figure 8 shows that the addition of the MMT concentration on the membrane tends to decrease the permeability value of membrane methanol. The addition of MMT concentration increases the membrane's crystallinity by dispersing MMT in the pore and matrix channels, thereby increasing the tortuosity and narrowing the methanol pathway through the membrane. The Si-O-Al bond on the stiff presses the polymer chains' space volume between the chitosan (García-Cruz et al., 2016). Besides that, the insoluble nature of PVA in alcoholic solutions makes methanol more difficult to pass through the membrane. This can be seen from the sharp decrease in the permeability of Cs when mixed with PVA. Based on Figure 8, the addition of 2% MMT became the lowest permeability value of methanol 1.43 x 10^{-7} cm^2 s^{-1}.

Furthermore, there was a sharp increase in the permeability of methanol on the membrane with a concentration of 4% MMT and continued to decrease until a concentration of 8% MMT. This is because the composition of MMT 2% is the composition of MMT, which is most suitable with the number of cross-links between chitosan so that MMT is well dispersed. The increase in methanol permeability at a concentration of 4% was caused by too many MMT particles trying to enter the cross-linking pores between chitosan. The pore cavities were not filled with MMT completely. The decrease in methanol permeability at 6% MMT and 8% MMT was further due to the increased crystallinity from the addition of montmorillonite concentrations.

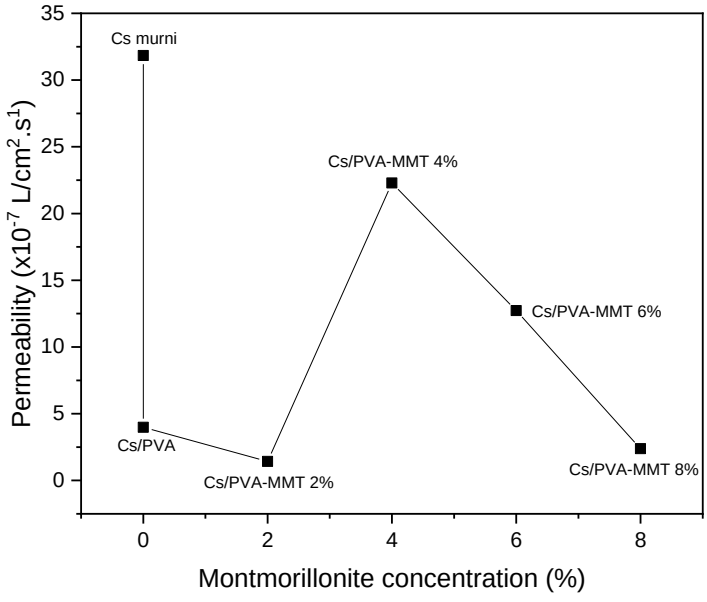

Figure 8 Graph of methanol permeability composite membranes

4. Conclusions

Research on the effect of montmorillonite (MMT) concentration on chitosan (Cs) composite membranes mixed with polyvinyl alcohol (PVA) with a ratio of Cs and PVA of 3: 1 w / w has been successfully carried out. The result is a membrane with a light brown physical appearance with a tougher texture than a pure Cs membrane. The addition of MMT concentrations tended to reduce water and methanol absorption. FTIR testing showed differences in absorption groups between pure Cs, Cs / PVA, and Cs / PVA-MMT membranes. In the methanol permeability test, it was found that the addition of the concentration in MMT tended to decrease the permeability of methanol, and the optimal concentration of MMT with the lowest methanol permeability was obtained, namely, at 2% MMT concentration, which had a methanol permeability value of 1.43×10^{-7} cm^2 s^{-1}.

In the analysis of water uptake and methanol uptake in general, the addition of montmorillonite concentration can increase the percentage of water uptake and reduce methanol uptake. The best water uptake value was obtained at a 4% MMT concentration, while the lowest methanol uptake value was obtained at 8% MMT concentration.

References

Cui, Z., Xing, W., Liu, C., Liao, J., & Zhang, H., 2009. Chitosan/heteropolyacid composite membranes for direct methanol fuel cell. *Journal of Power Sources*, 188(1), 24–29.

García-Cruz, L., Casado-Coterillo, C., Iniesta, J., Montiel, V., & Irabien, Á., 2016. Chitosan: poly (vinyl) alcohol composite alkaline membrane incorporating organic ionomers and layered silicate materials into a PEM electrochemical reactor. *Journal of Membrane Science*, 498, 395–407.

Guo, J., Li, X., Mu, C., Zhang, H., Qin, P., & Li, D., 2013. Freezing–thawing effects on the properties of dialdehyde carboxymethyl cellulose crosslinked gelatin-MMT composite films. *Food Hydrocolloids*, 33(2), 273–279.

Khan, A., Khan, R. A., Salmieri, S., Le Tien, C., Riedl, B., Bouchard, J., Chauve, G., Tan, V., Kamal, M. R., & Lacroix, M., 2012. Mechanical and barrier properties of nanocrystalline cellulose reinforced chitosan based nanocomposite films. *Carbohydrate Polymers*, 90(4), 1601–1608.

Khan, T.A., Peh, K.K., & Ch'ng, H.S., 2002. Reporting degree of deacetylation values of chitosan: The influence of analytical methods. *Journal of Pharmacy and Pharmaceutical Sciences*, 5(3), 205–212.

Lavorgna, M., Piscitelli, F., Mangiacapra, P., & Buonocore, G.G., 2010. Study of the combined effect of both clay and glycerol plasticizer on the properties of chitosan films. *Carbohydrate Polymers*, 82(2), 291–298.

Miyake, N., Wainright, J.S., & Savinell, R.F., 2001. Evaluation of a Sol-Gel Derived Nafion/Silica Hybrid Membrane for Polymer Electrolyte Membrane Fuel Cell Applications: II. Methanol Uptake and Methanol Permeability. *Journal of The Electrochemical Society*, 148(8), A905.

Neburchilov, V., Martin, J., Wang, H., & Zhang, J., 2007. A review of polymer electrolyte membranes for direct methanol fuel cells. *Journal of Power Sources*, 169(2), 221–238.

Palani, P.B., Abidin, K.S., Kannan, R., Sivakumar, M., Wang, F.-M., Rajashabala, S., & Velraj, G. 2014. Improvement of proton conductivity in nanocomposite polyvinyl alcohol (PVA)/chitosan (CS) blend membranes. *RSC Advances*, 4(106), 61781–61789.

Smitha, B., Sridhar, S., & Khan, A.A., 2006. Chitosan–poly (vinyl pyrrolidone) blends as membranes for direct methanol fuel cell applications. *Journal of Power Sources*, 159(2), 846–854.

Umar, S., Permana, D., & Atmaja, L., 2016. Effect of Glutaraldehyde Concentration Variation toward Properties and Performance of Composite Membrane (Chi-Mmt) for DMFC Application. *IPTEK Journal Proceedings Series*, 2(1), 199–200.

Wu, H., Zheng, B., Zheng, X., Wang, J., Yuan, W., & Jiang, Z., 2007. Surface-modifiedzeolite-filled chitosan membrane for direct methanol fuel cell. *Journal of Power Sources*, 173(2), 842–852.

Yang, J.M., & Chiu, H.C., 2012. Preparation and characterization of polyvinyl alcohol/chitosan blended membrane for alkaline direct methanol fuel cells. *Journal of Membrane Science*, 419, 65–71.

Journal of Membranes and Materials v(i) pp-pp (YYYY)
Received Month Year / Revised Month Year / Accepted Month Year

Journal of Membranes and Materials

https://ejournal2.undip.ac.id/index.php/jmm

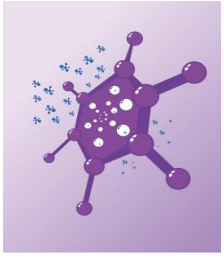

Removal of Total Suspended Solid and Polysaccharide in Seawater using Polysulfone Ultrafiltration Membrane

Nia Yusmaydiyanti[1,2*], Ria Desiriani[2], Yunita Fahni[2], Sudarno[1]

[1]*Department of Environmental Engineering, Faculty of Engineering, Diponegoro University, Jl. Prof. Soedarto, Tembalang, Semarang 50275, Indonesia*
[2]*Membrane Research Center, Integrated Laboratory for Research and Services, Diponegoro University, Jl. Prof. Soedarto, Tembalang Semarang 50275, Indonesia*

Abstract. The aim of this research measured the total removal of suspended solids and organic material in seawater using a polysulfone (PSf) ultrafiltration (UF) membrane. The results indicate that the salt concentration was significantly affected membrane flux. The lower flux of the membrane was obtained by a high content of the salt concentration. The fouling potential in decreasing the flux value was more dominant in the polysaccharide feed than the TSS feed. However, the fouling potential occurs more obviously in the mixed feed (TSS + polysaccharide), resulting in lower flux and higher rejection. PSf UF membranes successfully remove 93% of polysaccharides in a single feed, 95% in mixed feed, and 100% of suspended solids in a single feed and mixture.

Keywords: Polysaccharide; Polysulfone; Seawater; Total Suspended Solid

1. Introduction

Nowadays, many countries worldwide suffer from the scarcity of freshwater resources for industrial and agricultural purposes. Furthermore, several illnesses are associated with contaminated drinking water. To overcome this problem, seawater desalination is an alternative technology to produce freshwater (Khawaji et al., 2008). However, seawater cannot be consumed directly due to seawater has high inorganic and organic compounds (Ghaffour et al., 2013). Mostly, natural organic matter (Natural Organic Matter / NOM) in seawater can react easily with chlorine. Byproducts of the reaction are trihalomethanes (THMs), haloacetic acids (HAAs), and another halogenated organic that is carcinogenic. For this reason, seawater is necessary for treatment using some separation methods such as coagulation, flocculation, media filtration, and membrane process (microfiltration/ultrafiltration) (Vial et al., 2003).

Several studies have recently reported the high performance of MF/UF membranes as seawater pre-treatment (Ebrahim et al., 2001; Woo et al., 2015; Xu et al., 2010). Membrane technology is an efficient and cost-effective method to conventional separation processes. The pressure-driven membrane process was classified according to retain particle size into four categories such as microfiltration (MF), ultrafiltration (UF), nanofiltration (NF), and reverse osmosis (RO). MF and UF membrane has high performance in removing total suspended solids and organic material. However, the main problem of membrane usage is fouling. Therefore, fouling control is a crucial step in membrane used.

*Corresponding author's email: name@ai.ue.oa, Tel.: +00-00-000000; fax: +00-00-000000
doi: 10.14716/ijtech.v0i0.0000

In this study, the feed consist of a single feed of suspended solids (kaolin), a single feed of polysaccharides (sodium alginate), and a mixed feed of both (kaolin + sodium alginate). The specific studies in high salinity environments such as seawater, particularly with variations in the range of high salt concentrations (10,000 mg NaCl / L, 20,000 mg NaCl / L, and 30,000 mg NaCl / L) and varying salinity distributions have not been widely carried out. This research was measured the total removal of suspended solids (TSS) and polysaccharides in seawater using MF and UF membrane.

2. Methods

2.1. Materials

The polyethersulfone MF (MicroPES) and polysulfone UF (GR61PP) flat sheet membrane were used in this study. The flat sheet membrane had an MWCO of 0.04 – 0.12 µm and 20 kDa for MF and UF, respectively. NaCl, NaC6H7O6 (sodium alginate as a polysaccharide), C_6H_5OH, H_2SO_4 were purchased from Merck Inc., Germany. Kaolin as TSS was obtained from a local chemical store in Semarang.

2.2. Filtration system

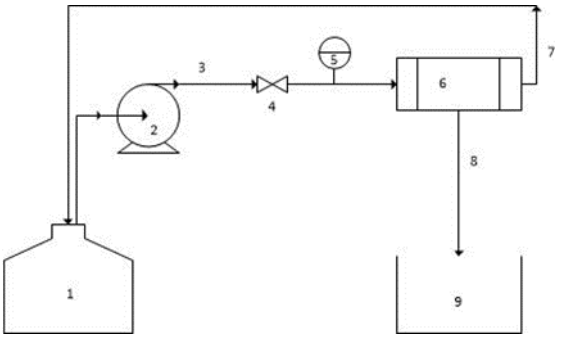

Figure 1 Schematic diagram of the membrane filtration system. (1: Feed tank, 2: Pressure pump, 3: Feed flow, 4: Valve, 5: Pressure gauge, 6: Membrane housing, 7: Concentrate flow, 8: Permeate flow, 9: Permeate)

A crossflow filtration set-up was used in the present study, as shown schematically in Fig. 1. The filtration experiment was conducted at a constant pressure of 0.5 bar and 1 bar for MF and UF membrane, respectively. Sodium alginate and kaolin (100 mg/l for MF and 10 mg/l for UF) were used as feed solution. Before the filtration, the membrane was compacted for 30 min. The permeate sample was gravimetrically 4 min interval. A small amount of samples were taken from the feed, permeate, and final concentrate for analysis.

2.3. Analytical methods

Sample from the feed, permeate, and concentrate was taken for the determined concentration of TSS and polysaccharide using spectrophotometry UV-Vis (Thermo Fisher Scientific, Genesys 20). Meanwhile, the presence of TSS and polysaccharide concentration by applied membrane process was showed in terms of % rejection and flux. The rejection of the main component was calculated using Equation (1):

$$R = 1 - \frac{C_p}{C_f} x100\% \quad (1)$$

Where C_p represents the concentration of a component in the permeate stream and C_f is the concentration of components in the concentrate stream. The permeate flux (J) is the volume of permeate collected per unit area membrane (A) and per unit time (t) as presented in Equation (2):

$$J = \frac{V}{Axt} \quad (2)$$

On the other hand, SEM (JEOL JSM-6510 LA) was used to observe the morphology of the fresh and fouled membrane surface. FTIR (Spectrum Two FTIR Spectrometer PerkinElmer, USA) measurements were used to analyze membrane top surface, and the recorded wavelength ranged between 400 and 4000 cm^{-1}.

3. Results and Discussion

3.1. Effect of Salt Concentration in Feed Solution on Membrane Performance

3.1.1. Salt Solution containing total suspended solids

Profiles flux (J_w/J_o) resulted with feed 100 mg/L kaolin for membranes Microfiltration Polyethersulfone (PES) filtration and 10 mg/L kaolin for Ultrafiltration membranes Polysulfone (PSf) filtration can be seen in Figure 2.

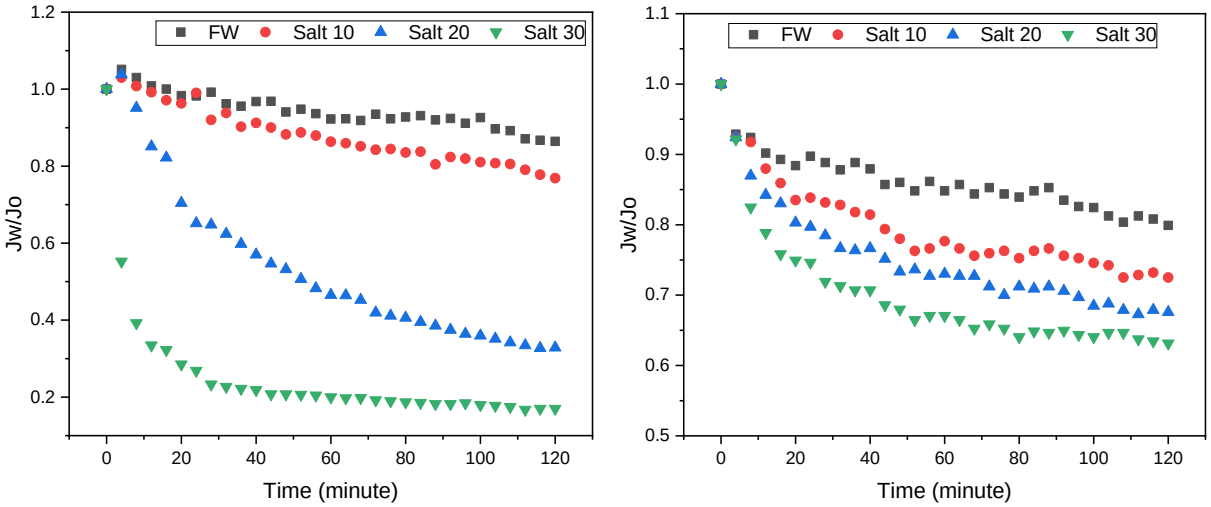

Figure 2 Profile flux of (a) 100 mg/l kaolin feed solution at various salt concentration using PES microfiltration membrane (b) 10 mg/l kaolin feed solution at various salt concentration using PSf ultrafiltration membrane

Figure 2 showed that, in general, the microfiltration and ultrafiltration membranes flux profile decreased during the operating time of 120 minutes. The lowest flux profile was on Salt 30 (30,000 mg salt solution of NaCl / L).

On Fresh Water (FW), kaolin likely to caused concentration polarization where kaolin covering the surface of the membrane. Concentration polarization was more easily swept away by the flow of crossflow. PSf ultrafiltration membranes flux profile decreased significantly by increasing salt concentration in the feed solution. From the pictures above, it appears that over time, a more dominant potential fouling occurred at higher salt concentrations. The higher the salt content, the more aggregates were formed and attached to the membrane's surface to lower the value of the flux profile. This founding was also consistent with Song and Singh (2005).

Under standard conditions with a plain water solution, kaolin always has a negative charge. The electrical double layer on the surface of the kaolin molecule initially led the negative charge into neutrality. That caused the decline of electrostatic repulsion between the kaolin and the membrane surface and supported kaolin's aggregation of the membrane's surface to form fouling.

TSS rejection in a single feed can be seen in Table 1.

Table 1 Number of receptors in each container

Permeate	TSS Rejection (%)	
	MF PES	UF PSf
Fresh Water	92.08	100
Salt 10	92.08	100
Salt 20	92.20	100
Salt 30	92.74	100

From Table 1, it can be seen that the membrane microfiltration PES can set aside TSS more than 92%, while for both ultrafiltration membrane can set aside 100%. The ability of membrane performance can explain this phenomenon. Ultrafiltration can remove the material with a smaller size.

Membrane pore size also affected the amount of rejection as Lau (2013) stated that the larger the pores, the lower the rejection rate. It caused due to the separation proceeds in the membrane was a sieving mechanism. It means that the particles in the feed with a smaller size than the membrane pores will escape, while particles larger than the membrane pores will be retained. Kaolin has a particle size of about 350 nm with a 100 kDa ≈ 10 nm (Jermann et al., 2007). This separation mechanism occurred either at the membrane surface or inside the membrane.

3.1.2. Salt Solution containing polysaccharide

Figure 3 shows the results for profile flux (J/J0) with a feed of 50 mg/L sodium alginate membranes Microfiltration Polyethersulfone (PES), and Ultrafiltration membranes Polysulfone (PSf).

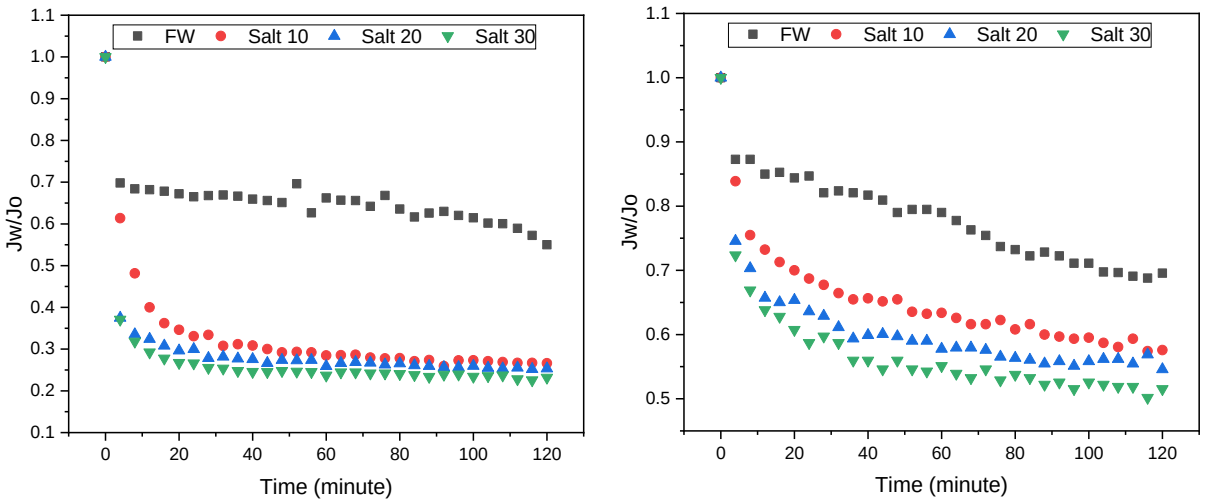

Figure 3 Profile flux of 50 mg/l sodium alginate feed solution at various salt concentration using (a) PES microfiltration membrane (b) PSf ultrafiltration membrane

Figure 3 showed that during the operating time of 120 minutes on each type of membrane, the flux profile decreased over time. The influence of collected particles on the surface of the membrane at the first minute was quite significant. As time went by, the foulant movement on the membrane surface was diminished. So its effect on reducing the flux profile was also reduced. The higher the salt content in the feed also gave a stronger effect on alginate fouling development, as a resulted flux profile also become lower. While in the microfiltration membrane, an increase in the salt concentration was not caused a significant decreased in the flux profile.

Resosudarmo et al. (2013) previously stated that a high salt concentration in sea water could significantly increase the potential fouling by organic material. Jermann et al. (2007) pointed out that sodium alginate membranes' interaction can produce strong electrostatic repulsion. That is

because both of them are negatively charged (Ven et al., 2008). The presence of ions, on the other hand, will greatly reduce the impact of the charge on the membrane, enhancing the contact between the membrane and the alginate molecules. It caused the electrostatic repulsion between molecules alginate and between molecule alginate-membrane surface to decrease (Lee et al., 2006; Ven et al., 2008 and Resosudarmo et al., 2012). According to Listiarin et al. (2011), salt's addition to a solution containing sodium alginate cause a gel formation that will increase the aggregate size of the sodium alginate. It explains how the effect of high saline conditions caused alginate fouling development during the filtration process.

Polysaccharide rejection in a single feed can be seen in Table 2.

Table 2 Polysaccharide rejection in a single feed

Permeate	Polysaccharide Rejection (%)	
	MF PES	UF PSf
Fresh Water	53.67	93.16
Salt 10	47.83	93.68
Salt 20	57.12	94.99
Salt 30	60.45	97.35

Table 2 shows that the PES membrane microfiltration can set aside approximately 50-60% sodium alginate, while both ultrafiltration membranes can set aside more than 85 percent sodium alginate. The sieving mechanism occurred during filtration using a membrane unit when the separation system was based on the membrane's pore size.

Sodium alginate has a molecular weight between 12-80 kDa (Jermann et al., 2009). Since the particle size of sodium alginate was similar to the ultrafiltration membrane's pore size, it was more effective to use ultrafiltration membranes to extract it. But it also contributed to a higher fouling potential as sodium alginate particles that accumulated near the surface of the membrane and surrounded the membrane pore able to degraded the membrane performance. On the other hand, the microfiltration membranes tend to pass sodium alginate molecules. However, the alginate's molecular weight can also be reached 0.20 µm. That enabled the MF membrane to restrain alginate molecules partially. Another problem that causes severe fouling was the adsorption of particles into the membrane, which downsizing the membrane pores.

3.1.3. Salt Solution containing total suspended solid and polysaccharide

Profiles flux (J / J0) were obtained using a feed of 100 mg / L kaolin + 50 mg / L sodium alginate membranes. Microfiltration is a term used to describe the method Ultrafiltration membranes with polyethersulfone (PES) and 10 mg/L kaolin + 50 mg/L sodium alginate.

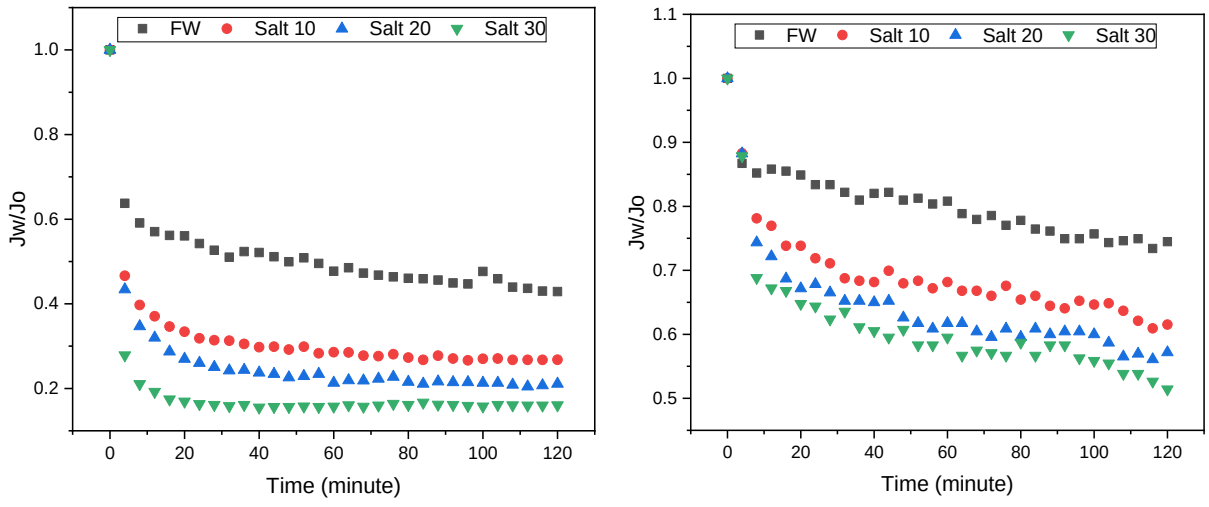

Figure 4 Profile flux resulted in 100 mg/l kaolin and 50 mg/l feed solution containing sodium alginate at various salt concentration using (a) PES microfiltration membrane (b) PSf ultrafiltration membrane

Figure 4 illustrates how the higher the salt content in the feed solution, the more robust the fouling effect on each membrane, resulting in a lower flux profile over time. The presence of sodium alginate and kaolin also raised the potential for greater fouling. The membrane with the mixed feed of kaolin and sodium alginate compared to the feed kaolin or sodium alginate only, the flux profile's tendency was similar to sodium alginate.

As already explained in the previous section how the interaction between the kaolin and sodium alginate with a high salt content resulted in a significantly decrease flux profile. It can be concluded fouling potential increased with the increasing salt concentration. Kaolin cake layer and alginate gel formation have resulted from the dense fouling from increasing salt concentration.

The feed stream with high ionic strength can compress the electrical double layer so that the electrostatic forces between particles were largely suppressed and non-electrostatic interactions become dominant (Motsa et al., 2015). The presence of sodium alginate and kaolin simultaneously produced thicker fouling on the membrane surface so that its rejection could be increasing. The deposition process of particles on the membrane surface will form a gel layer commonly referred to as a secondary membrane (Lopes et al., 2005). However, other things were also able to affect the rejection, such as molecules and membrane pore size.

Based on the results of the study, it showed rejection kaolin and polysaccharides in salt solution containing that mix feed can be seen in Table 3 and Table 4.

Table 3 Rejection kaolin in salt solution containing that mix feed

Permeate	TSS Rejection (%)	
	MF PES	UF PSf
Fresh Water	91.86	100
Salt 10	91.86	100
Salt 20	91.86	100
Salt 30	91.86	100

Table 4 Rejection polysaccharides in salt solution containing that mix feed

Permeate	Polysaccharide Rejection (%)	
	MF PES	UF PSf
Fresh Water	70.54	95.05
Salt 10	67.67	95.52
Salt 20	73.67	96.15
Salt 30	86.39	97.39

From Table 3 and Table 4 it can be seen that the membrane microfiltration PES can set TSS aside around 92%, while both of the ultrafiltration membranes can eliminate 100% of TSS. PES membrane microfiltration can be set aside around 70% for polysaccharides, while the average rejection for PSf ultrafiltration membranes was about 96%.

Based on Table 4 as compared to Tables 1 and 2, the rejection of sodium alginate on all membranes is higher in the feed mixture of kaolin with sodium alginate. The fouling formed on the membrane surface is greater, built up as a secondary layer. Ion concentration in the feed can also affect rejection, as described in the previous section, where the higher concentration of ions then will increase fouling development.

3.2. Effect of TSS for Ultrafiltration Membrane Performance

The addition of kaolin, as in the previous discussion, may lead to concentration polarization or aggregates' formation. Based on the results of the comparison to the MF filtration, it can be

seen that the flux profile with feed kaolin (mixture) decreased lower than feed without kaolin (only sodium alginate). However, filtration UF showed opposite results. Profile flux both coincide; even with flux profile of kaolin mixture solution tends to be above the solution without kaolin. It showed that a small amount of kaolin concentration in UF filtration (10 mg/l) did not significantly influence. To prove this assumption, test flux with the addition of kaolin mixed solution of 50 mg/l in the salt solution (30,000 ppm NaCl) and FW (Freshwater / Water Flute). The flux profile results were compared to the addition of kaolin mixed solution 0 mg / l and 10 mg / l.

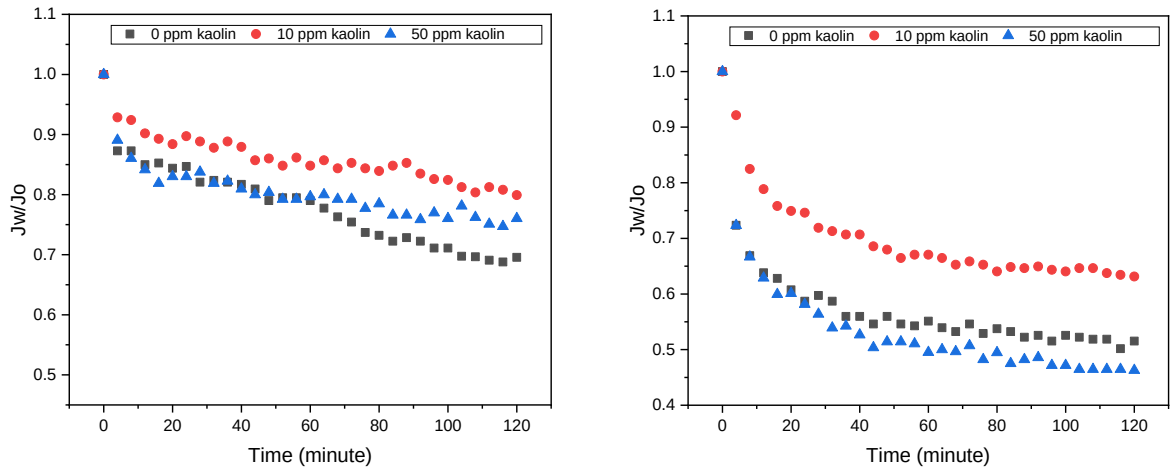

Figure 5 Profile flux with feed solution; Sodium Alginate, Kaolin, and Mixed in Fresh Water using (a) PES microfiltration membrane (b) PSf ultrafiltration membrane

According to the flux profile test results on both UF membranes in fresh water (see Figure 5), all feed solutions with 0 ppm kaolin (sodium alginate feed only), 10 ppm kaolin, or 50 ppm kaolin had a higher flux profile than the salt solution. Unlike in the salt solution, the decline in flux profile becomes a bit lower as the higher kaolin concentration was added.

A decreased in the flux profiles at both UF membranes between the concentration of a single feed to a mixture of 10 ppm kaolin in salt solution was so small that there's no significant difference in the results. It can occur because the kaolin feed concentration was very small, so it was more easily swept away by the crossflow and did not contribute to fouling. But after kaolin was added to 50 ppm in salt solution feed, the flux profile on the membrane filtration was significantly lower. It was consistent with Jermann et al. (2007), which states that the flux profiles with a feed mix will contribute to greater fouling than a single feed. These results were also consistent with previous research, which states that the reduction in profile flux significantly demonstrated by the fouling combination between colloidal silica and organic material in connection with the increase in osmotic pressure at the membrane surface (Lee et al., 2005; Li and M. Elimelech., 2006).

Table 5 Rejection TSS and polysaccharides in freshwater containing that mix feed

Kaolin	Rejection (%)	
(mg/L)	TSS	Polysaccharide
0	100	93.16
10	100	-
50	100	95.42

Table 6 Rejection TSS and polysaccharides in salt solution containing that mix feed

Kaolin	Rejection (%)

(mg/L)	TSS	Polysaccharide
0	100	97.35
10	100	-
50	100	97.64

Based on Table 5 and Table 6 for PSf ultrafiltration membrane, the rejection of sodium alginate increased with the addition of kaolin in the feed solution, followed by a decline in flux profile. On filtration in a salt solution, adding kaolin with higher concentrations did not increase the rejection of sodium alginate through flux profile also decreased, indicating increased fouling potential—besides, the rejection in freshwater also greater than the salt solution. In contrast, a decrease in the freshwater flux profile is lower than the saline solution.

When their alginate molecules are trapped in a kaolinite structure, they can not diffuse back (Jermann et al., 2007). According to Jermann, it will intensify the alginate-pore blocking and adsorption on the membrane. It also allowed the alginate molecules smaller than the pore membrane to permeate to pass together. It explained the phenomenon of lower rejection in sharper declined flux profile in the salt solution. As for the phenomenon that occurred in freshwater, this may be caused by the cross-flow as described earlier. So it was possible to maintain high profile flux and greater rejection value in the freshwater feed solution.

3.3. Fouling characterization on the ultrafiltration membrane surface

3.3.1. Fourier Transform Infrared Spectroscopy (FTIR)

FTIR test was to find out the fouling composition on the membrane surface. Figure 6 shows the FTIR test results for polysulfone ultrafiltration membranes with sodium alginate feedback on Fresh Water and 30,000 mg NaCl / L Salt Solution.

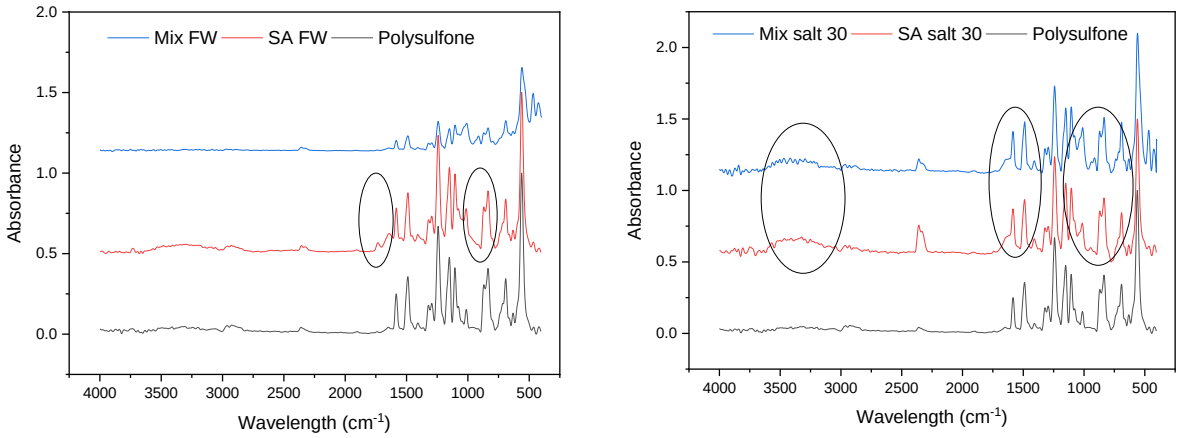

(a) (b)

Figure 6 The FTIR result of polysulfone ultrafiltration membranes with sodium alginate feedback (a) Fresh Water (b) Salt Solution.

The presence of peaks of unique wavelengths can be seen in the four figures above, with the most important peak occurring in salt solution as compared to freshwater, which is the area about 3500-3200 cm^{-1}, which indicates the presence of hydroxyl groups (OH) bonded to hydrogen, and at 3100-3000 cm^{-1}, which indicates the presence of aromatic groups (CH). Wavenumber 1760-1665 cm^{-1} indicate the presence of a carbonyl group (C = O) as the aromatic group, 1680-1640 shows the alkene group (-C = C-), 1600-1585 cm^{-1} shows an aromatic group (CC), 1320- 1000 cm^{-1} indicates the presence of carboxyl group (CO). The alginate, according to Mury et al. (2005) in Mutia et al. (2011), is a natural polymer with aromatic groups (ROR) containing -OH, -COOH and -CH, -C = C- and -C = O. Isomer of sodium alginate lies in the absorption peak in 1614 cm^{-1} and 1431 cm^{-1}. According to Stuart (2004), the presence of an OH group in the 3800-3400 cm^{-1} range for kaolin and Si-O groups in the 1300-400 cm^{-1} range for kaolin indicate the presence of

OH stretching and bending. The content of Al (III) in the kaolin will form a strong bond at 1120-1000 cm^{-1} region. Thus, the results obtained FTIR spectra showed that the fouling caused by sodium alginate is more dominant in the feed salt solution was 30,000 mg NaCl / L compared with Fresh Water.

3.3.2. Scanning Electron Microscopy (SEM)

SEM analysis showed the form and change in surface morphology of the samples analyzed. In polysulfone ultrafiltration membrane filtration, the fouling behavior of each foulant was revealed by SEM results. The results of filtration by PSf ultrafiltration membrane are presented in the figures below.

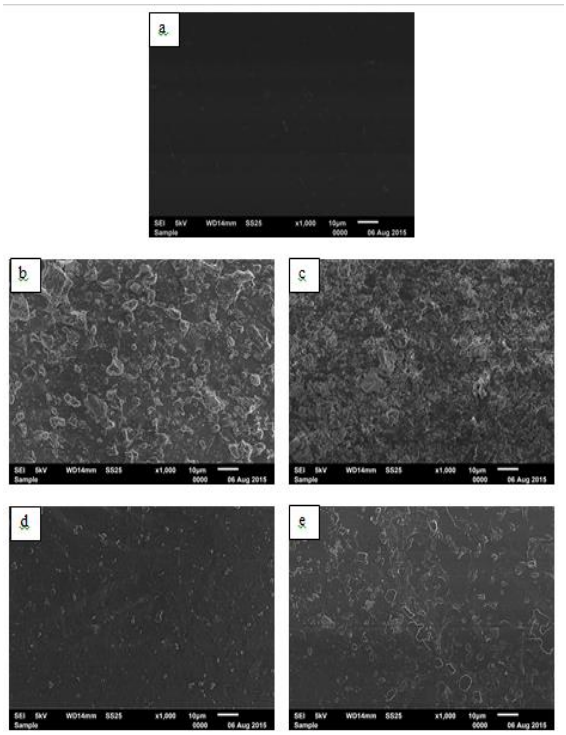

Figure 7 UF Membrane SEM results in Polysulfone Filtration; a] New Membrane; b] Mix (sodium alginate 50 ppm and 10 ppm kaolin) in Salt 30; c] 50 ppm Sodium Alginate in Salt 30; d] Mix (sodium alginate 50 ppm and 10 ppm kaolin) in FW; e] 50 ppm Sodium Alginate in FW

By comparing all the figures above, it showed the difference between the results of SEM before filtration membrane with the membrane after filtration using a solution of a mixture of kaolin and sodium alginate and a single sodium alginate solution. Different phenomena showed on the condition of Fresh Water. With a solution of salt 30,000 mg NaCl/L, the presence of high salt content caused the foulant to bind to each other and formed aggregates that produced more large effect fouling compared to normal conditions (Fresh Water).

In the mixed feed, it appeared that the accumulated fouling on the membrane surface was a more dominant place in the kaolin mixture with sodium alginate compared with a single sodium alginate solution. In the salt solution, a fouling layer formed more likely to have a larger structure. It can be caused due to the condition of ionic, kaolin, and sodium alginate more easily bind to form aggregates (enlarge molecular structure). With a high ion condition, kaolin can adsorb sodium alginate, absorbed by the membrane surface or into the membrane's pores. The presence of kaolin adsorption with sodium alginate was the main caused of the formation of the cake layer. It was more dominant on the surface of the membrane with a feed salt solution. This assumption was by Zularisam et al. (2011), which states that the organic material will form the structure of the fouling layer that serves as the "glue" for inorganic constituents.

For single sodium alginate solution feed on Fresh Water showed that sodium alginate was spread evenly on the surface of the membrane and is not mutually bonded to one another in the absence of the influence of ions affects the charge, respectively. The addition of salt causes more complex alginate molecules formation because it reduced the charge's effect in the alginate molecules. It also caused more entanglement of the polymer chains that were more complex and increased the alginate molecules' density. The interaction between the membrane and alginate molecules caused pore blocking or narrowing pore, but based on its main properties can also form a gel layer on the membrane surface. Sodium alginate gel structure was formed on the membrane's surface depending on the ionic environment (Ven et al., 2008).

Fouling behavior by kaolin and sodium alginate in different environments can be described in the figure below.

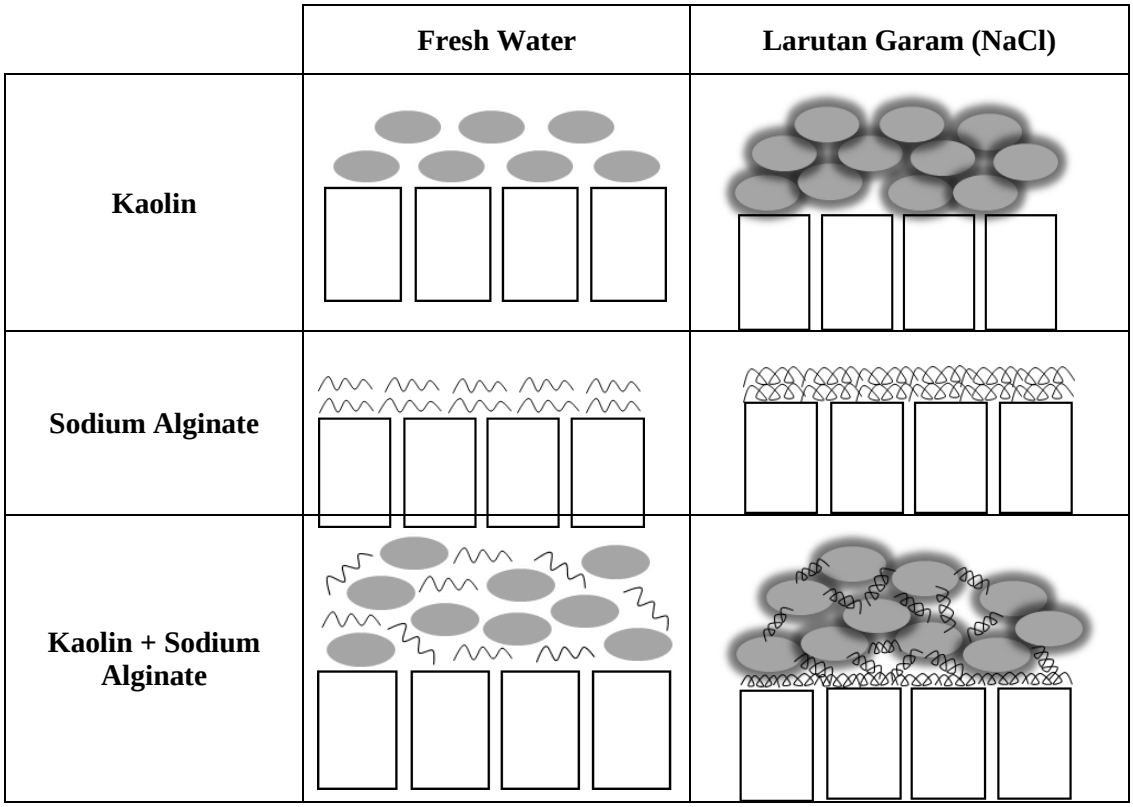

Figure 8 The Fouling phenomenon is illustrated by Sodium Alginate and Kaolin in different environments

4. Conclusions

Polysulfone ultrafiltration membrane removes total suspended solid and polysaccharide in seawater effectively. It is evidenced by the high resulting polysaccharide rejection in the synthetic seawater. PSf UF membranes successfully remove 93% of polysaccharides in a single feed, 95% in mixed feed, and 100% of suspended solids in a single feed and mixture. However, the fouling potential occurs more obviously in the mixed feed (TSS + polysaccharide), resulting in lower flux and higher rejection.

References

Ebrahim, S., Abdel-Jawad, M., Bou-Hamad, S., Safar, M., 2001. Fifteen Years of R&D Program in Seawater Desalination at KISR Part I. Pretreatment Technologies for RO Systems. *Desalination*, 135, pp. 141–53.

Ghaffour, N., Missimer, T.M., Amy, G.L., 2013. Technical Review and Evaluation of the Economics of Water Desalination: Current and Future Challenges for Better Water Supply Sustainability. *Desalination*, 309, pp. 197–207.

Jermann, D., Pronk., W., Kagi, R., Schaarschmidt, N., Halbeisen, M., Boller, M., 2008. Influence of Particles on UF Fouling by NOM – Rethinking The Perception Of NOM Fouling. *Water Research*, 42, pp. 3870 – 3878.

Jermann, D., Pronk, W., Boller, M., Schäfer, A.I., 2009. The Role of NOM Fouling on The Retention of Estradiol and Ibuprofen During UF For Drinking Water Production. *Journal of Membrane Science*, pp. 329, 75-84.

Khawajia, A.D., Kutubkhanah, I.K., Wie, J., 2008. Advances in Seawater Desalination Technologies. *Desalination*, 221 (1–3), pp. 47–69.

Lau, W. J., Ismail., A.F., Firdaus, S., 2013. Car Wash Industry in Malaisya: Treatment of Car Wash Effluent Using Ultrafiltration and Nanofiltration Membranes. *Separation dan Purification Technology*, 104, pp. 26-31.

Lee, S., Ang, W.S., Elimelech, M., 2006. Fouling of RO Membrane by Hydrophilic Organic Matter Implications for Water Reuse. *Desalination*, 187 (1-3), pp. 313-321.

Li, Q., and Elimelech, M., 2006. Synergistic Effects in Combined Fouling of a Loose Nanofiltration Membrane by Colloidal Materials and Natural Organic Matter. *Journal of Membrane Science* 278, pp. 72–82.

Lopes, C.N., Petrus, J.C.C., Riella, H.G., 2005. Color and COD Retention by Nanofiltration Membranes. *Desalination*, 172, pp. 77-83.

Listiarin, K., Chun, W., Sun, D.D., Leckie, J.O., 2009. Fouling Mechanism and Resistance Analyses of System Containing Sodium Alginate, Calcium, Alum and Their Combination in Dead End Fouling of Nanofiltration Membranes. *Journal of Membrane Science*, 344, pp. 244-251.

Motsa, M.M., Mamba, B.B., Verliefde, A.R.D., 2015. Combined Colloidal and Organic Fouling of FO Membranes: The Influence of Foulant–Foulant Interactions and Ionic Strength. *Journal of Membrane Science,* 493, pp. 539–548.

Mutia, T. Rifaida E., Ratu S. 2011. Membran Alginat sebagai Pembalut Luka Primer dan Media Penyampaian Obat Topikal untuk Luka yang Terinfeksi. Jurnal Riset Industri, Vol. V, No.2, Hal 161-174.

Resosudarmo, A., Ye, Y., Le-Clech, P., Chen, V., 2013. Analysis Of UF Membrane Fouling Mechanisms Caused By Organic Interactions In Seawater. *Water Research,* 47, pp. 911-921

Baltasar, P., and García-Rodríguez, L., 2012. Current Trends and Future Prospects in the Design of Seawater Reverse Osmosis Desalination Technology. *Desalination*, 284, pp. 1–8.

Song, L., and Singh, G., 2005. Influence Of Various Monovalent Cations And Calcium Ion On The Colloidal Fouling Potential. *Journal of Colloid and Interface Science,* 289, pp. 479–487.

van de Ven, W.J..C., van't Sant, K., Pünt, I.G.M., Zwijnenburg, A., Kemperman, A.J.B., van der Meer, W.G.J., Wessling, M., 2008. Hollow Fiber Dead-End Ultrafiltration: Influence Of Ionic Environment On Filtration Of Alginates. *Journal of Membrane Science*, 308, pp. 218-229.

Vial, D., and Doussau, G., The Use of Microfiltration Membranes for Seawater Pre-Treatment Prior to Reverse Osmosis Membranes. *Desalination*, 153 (1–3), pp. 141–47.

Woo, Y.C., Lee, J.J., Tijing, L.D., Shon, H.K., Yao, M., Kima, H-S., 2015. Characteristics of Membrane Fouling by Consecutive Chemical Cleaning in Pressurized Ultrafiltration as Pre-Treatment of Seawater Desalination. *Desalination*, 369, pp. 51–61.

Xu, J., Chang, C-Y., Gao, C., 2010. Performance of a Ceramic Ultrafiltration Membrane System in Pretreatment to Seawater Desalination. *Separation and Purification Technology*, 75, pp. 165–73.

Zularisam, A.W., Ahmad, A., Sakinah, M., Ismail., A.F., Matsuura, T., 2011. Role of Natural Organic Matter (NOM), Colloidal Particles, and Solution Chemistry on Ultrafiltration Performance. *Separation and Purification Technology*, 78, pp. 189-200.

Journal of Membranes and Materials v(i) pp-pp (YYYY)
Received Month Year / Revised Month Year / Accepted Month Year

Journal of Membranes and Materials

https://ejournal2.undip.ac.id/index.php/jmm

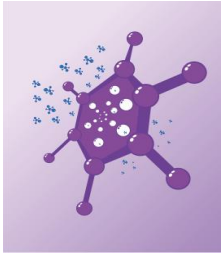

Separation of Saponin Using Nanofiltration Membrane

Nur 'Aini Hamada[2*], Ilham Dwiyanto Emzar[1,2], Yuniar Luthfia Listyadevi[1,2]

[1]*Department of Chemical Engineering, Faculty of Engineering, Diponegoro University, Jl. Prof. Soedarto, Tembalang, Semarang 50275, Indonesia*
[2]*Membrane Research Center, Integrated Laboratory for Research and Services, Diponegoro University, Jl. Prof. Soedarto, Tembalang Semarang 50275, Indonesia*

Abstract. Separation of pure saponin and saponin-BSA protein mixture by nanofiltration membranes have been investigated in this study to understand the nanofiltration potential to obtain high purity saponin. Commercial NF membranes: NF, NF270, and DSS-ETNA01PP were used. The effects of the operating conditions such as pressure, the concentration of feed, and the composition of feed were evaluated. The permeate flux and rejection rate of saponin and saponin-BSA were the criteria of this evaluation. The increasing operating pressure increased the permeate flux. In addition to the membranes' MWCO, electrostatic repulsion between the charged membrane interface and solute determined the saponin and saponin-BSA solution's rejection rate. The flux of pure saponin feed was greater but generated lower rejection rates than the saponin-BSA feed. Increasing feed concentration resulted in an increased rejection rate. However, the flux decreased with increasing pure saponin concentration but increased with a higher dose of saponin-BSA. The DSS-ETNA01PP membrane had the largest flux value and the smallest rejection value compared to other membranes. The results indicated that nanofiltration was potential for the saponin purifying process.

Keywords: Electrostatic; Nanofiltration; Rejection; Repulsion

1. Introduction

Saponins are secondary metabolic products found in plants with high molecular weight. Saponins can be found in dicot and monocot plants, including *Camellia sinensis*, *Aesculus hippocastanum*, *Rosa centifolia*, *Swietenia mahogany*. Saponins function as chemical barriers or protectors in plant self-defense systems against pathogenic bacteria and herbivores (Augustin et al., 2011). Saponins are composed of sugar units linked to triterpene or steroid aglycones. Saponins generally have detergent-like properties, reducing the surface tension in aqueous solutions and forming a stable foam. Saponins can dissolve in various solvents such as water, ethanol, and methanol. It is partly soluble in ether, chloroform, benzene, ethyl acetate, or acetic acid (Hostettmann and Marston, 1995).

Saponins are widely used in the cosmetics, agriculture, food, and pharmaceutical industry. They have hemolytic, anti-inflammatory, anti-yeast, antimicrobial, antiparasitic, anti-tumor, and antiviral properties (Sparg et al., 2004). The discovery of saponins' biological activity triggered the semi-synthesis of steroid drugs in the pharmaceutical industry.

With the increasing use of saponins, many studies have been conducted to obtain commercial-scale saponins from plants (Guclu-Untundag and Mazza, 2007). The most used attempt is by carrying out extraction, which several methods can do, including maceration

*Corresponding author's email: nurainih@live.com, Tel.: +62-857-0095-2496
doi: 10.14716/ijtech.v0i0.0000

(Takeuchi et al., 2009), reflux and soxhlet (Bart, 2011), ultrasonic (Wu et al., 2001), and microwave (Vongsangnak, 2004).

However, the extracted saponin content is still insufficient, so further purification steps are needed to obtain high saponin content (Guclu-Untundag and Mazza, 2007). The saponin purification process can be conducted in several ways, including solvent precipitation (Kitagawa, 1986; Nozomi et al., 1986), adsorption (Giichi, 1987), and chromatography (Kensil and Marciani, 1991). Chromatography is often used in laboratory-scale saponin purification processes such as open column chromatography, thin-layer chromatography (TLC), liquid chromatography, and countercurrent chromatography (Hostettmann and Marston, 1995). However, commercial-scale saponin production using this method is not economical (Guclu-Untundag and Mazza, 2007).

Another method that can be applied for saponin purification is nanofiltration. This technology does not require additional chemicals, operates isothermally at room temperature, and consumes low energy (Susanto, 2009). Nanofiltration membranes procure very high rejections for multivalent ions (>99%), low to moderate rejections for monovalent ions (0–70%), and high rejection (>90%) for organic compounds with a molecular weight above the membrane's (Norman et al., 2008).

This study aimed to discover the potential of nanofiltration membranes for obtaining high purity saponins. The membranes' performance and characteristics would be assessed for the process with various membrane types, pressures, feed compositions, and feed concentrations.

2. Methods

2.1. Materials

The materials used in this study were saponins (Sigma Aldrich, 8-25%), BSA protein (Sigma Aldrich, ≥98%), vanillin (Sigma Aldrich, 99%), H_2SO_4 (Sigma Aldrich, 96 %). The membranes used were NF (Alfa Laval), NF270 (FILMTEC), and DSS-ETNA01PP (Alva Laval).

2.2. Flux Measurement

The membrane was cut with a diameter of 4.2 cm, then soaked for 30 minutes in distilled water. The membrane was inserted into the membrane module and compacted for 30 minutes with pressure above the operating pressure (5, 6, 7 bar). The feed was filled with distilled water. The distilled water flowed through the filtration unit for 15 minutes at operating pressure (4, 5, 6 bar) to obtain J_0. Afterward, the permeate was collected and weighed. Then, the saponin feeds (pure/mixed with BSA) were put in the feed tank, filtered for 2 hours at specific operating pressures. The permeate was collected and weighed every 15 minutes to measure the flux.

2.3. Rejection Analysis

The rejection analysis was done spectrophotometrically. The water was heated to 60°C. Five ml of 72% H_2SO_4 solution was put in a container covered with aluminum foil. Vanillin solution of 8% w/v was made. Half ml of it was put in the container containing H_2SO_4 solution and rested for 1 minute. Half ml of permeate from the filtration process was added into the container containing vanillin and H_2SO_4 mixture and rested for a minute. The container was then heated for 10 minutes in hot water and cooled in the ice water for 5 minutes. The mixture's absorbance was measured using a spectrophotometer (Genesys 20) at the wavelength of 544 nm.

3. Results and Discussion

3.1. Effect of Pressure on Flux in NF270 and DSS-ETNA01PP Membrane

The filtration process of pure saponin and saponin-BSA protein with operating pressures of 4, 5, and 6 bar using NF270 and DSS-ETNA01PP membranes was done to investigate the effect of pressure on flux. The feed concentrations were varied from 50, 100, to 150 ppm. The results can be seen in Figure 1.

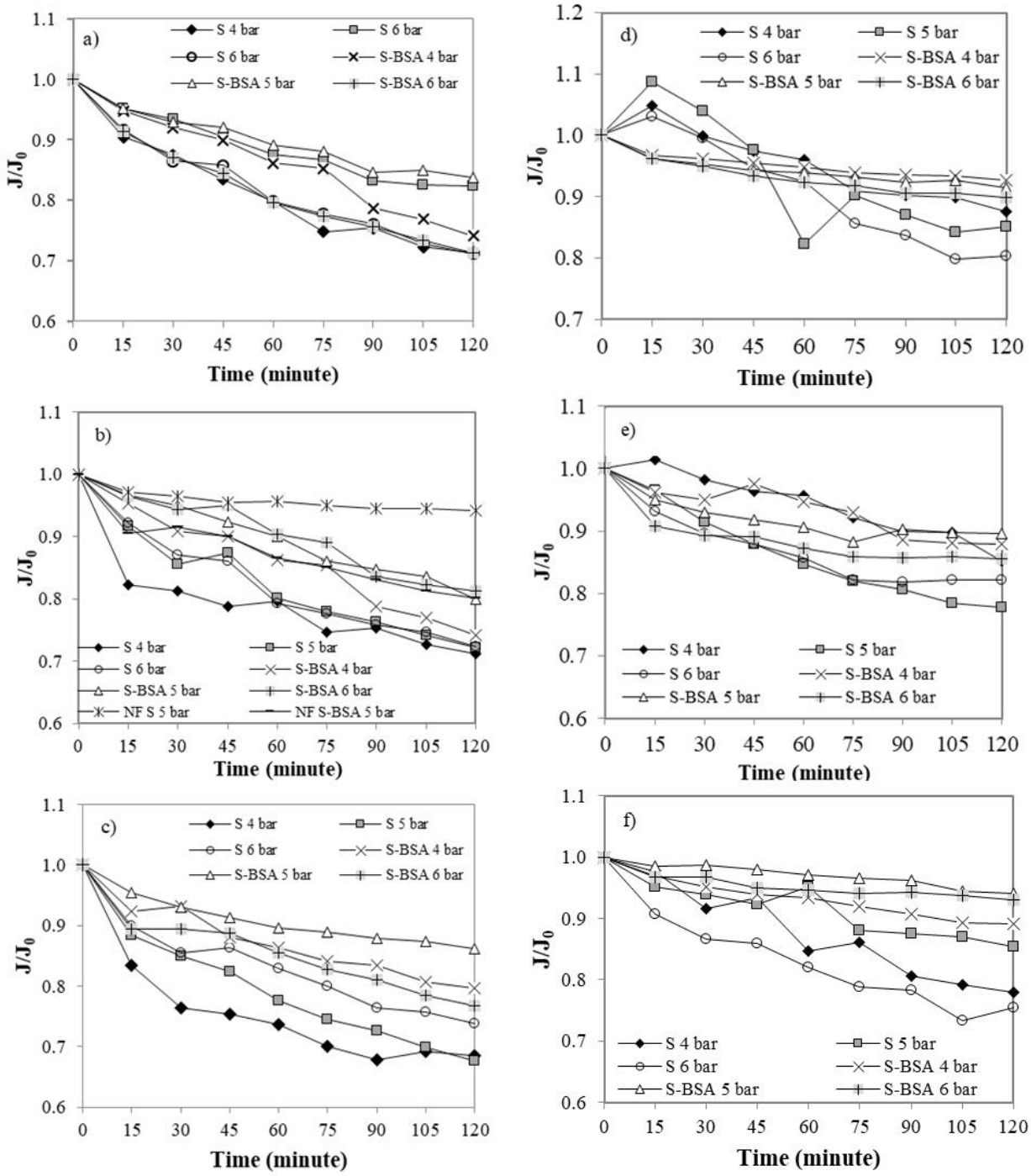

Figure 1 Flux profiles of various feed concentrations: a) NF270-50 ppm, b) NF270-100 ppm, c) NF270-150 ppm, d) DSS-ETNA01PP-50 ppm, e) DSS-ETNA01PP-100 ppm, f) DSS-ETNA01PP-150 ppm

Figure 1 shows that the flux profile decreased with a longer operating time on both membrane types. The flux drop was relatively consistent with each pressure variation. For NF270, the flux of 5 bar had the most optimal value than of 4 and 6 bar at 50 ppm. On the other hand, at the concentration of 100 ppm and 150 ppm, there was no significant difference in each pressure variation's flux.

The pressure of 4 bar resulted in the smallest flux; this was because the crossflow's driving force was less significant. So that the molecules accumulated on the membrane surface were not swept away by the recycle flow.

The flux reduction using the DSS-ETNA01PP membrane was relatively consistent at each pressure variation. As the filtration operation time increased, the resulting flux also decreased and became more stable at the end of the operation time. This phenomenon occurred both in pure saponin and saponin-BSA feed.

Mixed feed solution of saponin and BSA showed increased flux value with increasing operating pressure. At a pressure of 6 bar, the resulting flux was higher compared to other operating pressures because the driving force applied was more significant so that more solutions could pass through the membrane.

According to Lin et al. (2004), the decrease in normalized flux occurred due to fouling and polarization concentration on the membrane surface. Besides, protein molecules' nature is easily adsorbed by membrane surfaces and pores, making BSA a foulant that is quite difficult to control (Wei et al., 2006). The longer the operating time, the more BSA would be deposited on the membrane's surface and pores. It resulted in the flux decrease.

As the operating time increased, the resulting flux decreased, while at the end of the operating time, the flux value became more stable. This phenomenon was caused by fouling and polarization concentration on the membrane surface. Fouling is the deposition of suspended substances, usually solutes, which results in decreased membrane performance and is irreversible. Meanwhile, polarization concentration occurred due to solute accumulation that stuck on the membrane surface, so that it caused flux decrease and is reversible (Lin et al., 2004; Sutzkover-Gutman et al., 2010).

In this saponin filtration, fouling occurred because of the sieving mechanism—the molecule size difference between the solute molecules and the membrane pore size caused the separation process. Saponin compounds have a molecular weight of 414.63 Da, and BSA has a molecular weight of 66,430 Da. Meanwhile, the pore size or Molecular Weight Cut Off (MWCO) of the NF-270 membrane is 180 Dalton. Theoretically, saponin compounds and BSA protein compounds would be stuck on the membrane surface because they had a larger molecular size than the membrane pores. As the filtration operation time increased, more molecules would cause fouling on the membrane, resulting in the flux decreasing.

3.2. Effect of Pressure, Feed Composition, and Feed Concentration on Rejection Rate

Pure saponin and saponin-BSA protein filtration processes using NF, NF270, and DSS-ETNA01PP were done to investigate the effect of pressure on rejection rate. The operating pressures were 4, 5, and 6 bar while the feed concentrations were 50, 100, and 150 ppm. The results are presented in Table 1.

The pure saponin solution feed that passed on the NF270 membrane showed that the higher the feed concentration, the greater the rejection rate. Pedebos et al. (2014) reported that carboxyl groups in saponin made the feed solution negatively charged. The NF membrane's surface has been known to be negatively charged. As the concentration of the solution increased, the number of saponin molecules would also increase. It resulted in greater repulsion force (electrostatic repulsion) between the membrane surface and the solution. Therefore, the higher saponin feed concentration increased the rejection rate of the NF270 membrane.

In the saponin-BSA mixed feed, the rejection data show an increase in the rejection rate from 50 ppm to 100 ppm then slightly decreased at a concentration of 150 ppm. The increase in rejection rate was caused by electrostatic repulsion from the membrane surface and solute interaction. In a study conducted by Chaiyasut and Tsuda (2001), the BSA molecule had an isoelectric point at pH 4.6-4.7. It is a condition where the BSA molecule's net charge is zero (Salgin et al., 2012). In this study, the saponin-BSA mixed feed solution pH was above 5, indicating that the BSA molecule was negatively charged. Therefore, the electrostatic repulsion became more significant with increasing feed concentration, resulting in a higher rejection rate.

Table 1 Rejection Rate of the Membranes

Membrane	Feed	Concentration	% Rejection		
			4 bar	5 bar	6 bar
NF270	Pure Saponin	50 ppm	23.3	21.6	24.4
		100 ppm	35.9	30	31.1
		150 ppm	56.8	55	43
	Saponin - BSA	50 ppm	43.8	41	40
		100 ppm	74	70.5	67
		150 ppm	73.7	68.7	62.5
NF	Pure Saponin	100 ppm	N/A	55.5	N/A
	Saponin - BSA		N/A	63.4	N/A
DSS-ETNA01PP	Pure Saponin	50 ppm	40.7	57.1	60.5
		100 ppm	31.7	60.5	71.6
		150 ppm	33.7	41.2	53
	Saponin - BSA	50 ppm	33.8	35.3	29.4
		100 ppm	52	48.1	29.4
		150 ppm	52	63.9	59.8

At the same operating condition, the rejection rate of the saponin-BSA mixture feed was greater than the pure saponin feed. Carvalho et al. (2011) reported that the membrane and ionic charges in the solution provided additional rejection because of the electric and dielectric effects. Thus, apart from the sieving mechanism effect, saponin separation on the NF membrane also occurred through an electrostatic repulsion mechanism. The NF membrane's surface and the pure saponin solution were negatively charged, inducing repulsive force.

Saponin-BSA mixture was more negatively charged than the pure saponin, creating greater electrostatic repulsion that generated a higher rejection rate and increasing feed concentration.

The rejection data of filtration using DSS-ETNA01PP membrane in Table 1 shows a decrease in rejection rate with increasing pure saponin solution feed concentration. Meanwhile, the saponin-BSA mixture filtration's rejection rate had the opposite phenomenon with the pure saponin feed. As the mixed feed concentration increased, the resulting rejection also increased. It was because the saponin-BSA mixed solution had different properties than the pure saponin. Kezwon and Wojciehjowski (2014), in their research on saponin-protein interactions in food, concluded that saponins would aggregate with protein molecules due to the saponin properties, which could reduce surface tension and also had a high aggregation behavior. Based on these properties, the higher the solute concentration in the feed solution, the more molecules would form the aggregates resulting in a wider molecular diameter. With a wider molecular diameter, theoretically, it could not pass through the smaller membrane pores. Therefore, the rejection rate would increase as the concentration of the saponin-BSA mixture feed increased.

3.3. Characterization of membrane fouling

SEM analysis is one way to characterize membrane fouling from the membrane surface and membrane pore cross-sections. The SEM test results of the three membranes used to filter pure saponin solution and saponin-BSA protein solution are presented in Figure 2.

According to Figure 2, there was no significant difference seen in both the membrane used to filter pure saponin and saponin-BSA protein. There was fouling on both used membranes indicated by oval-shaped molecules, which belonged to saponins. In the membrane used to filter saponin-BSA protein solution, round molecules were seen, representing the BSA protein. If we

look at the cross-section SEM analysis results, the used DSS-ETNA01PP membranes had the largest pores shaped like fingers.

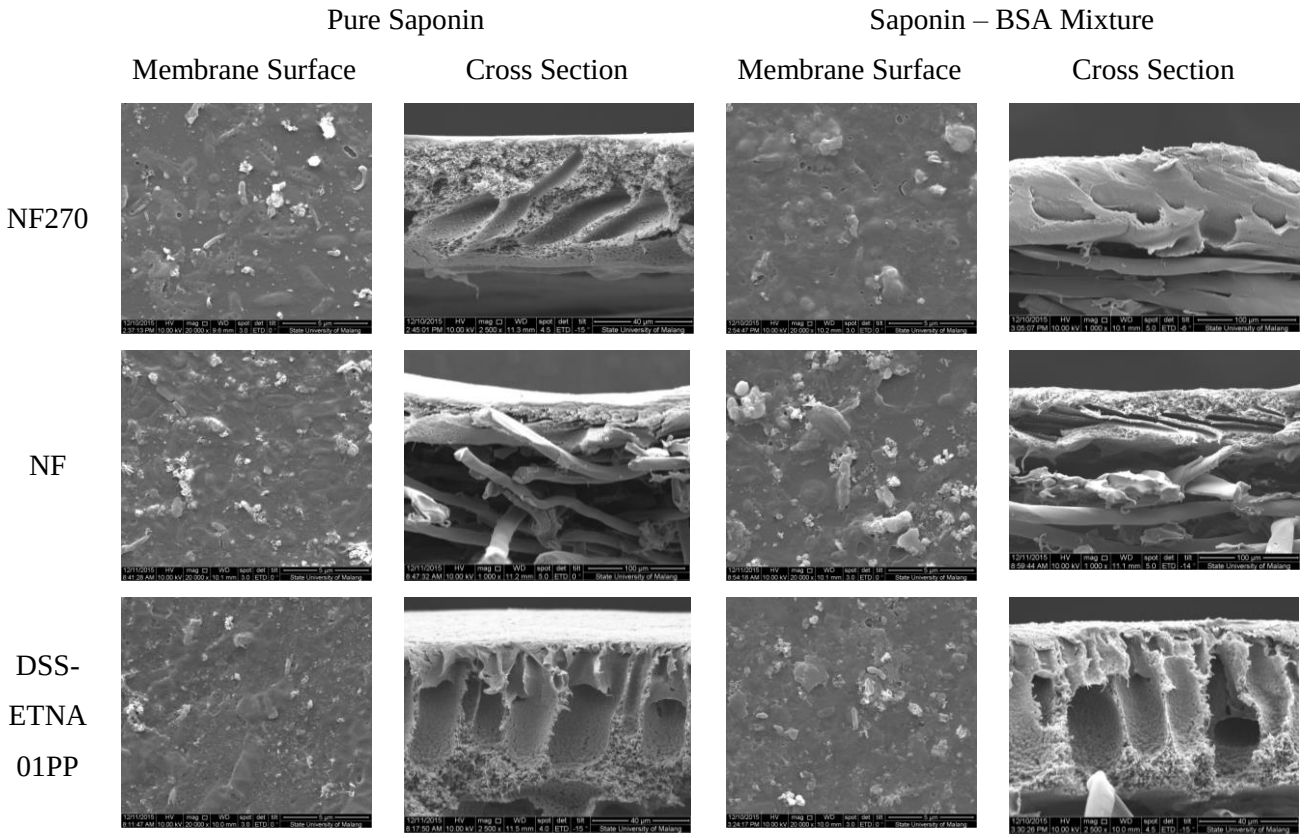

Figure 2 SEM characterization of the membranes used to filter 100 ppm of pure saponin and saponin-BSA protein

4. Conclusions

This research aimed to know the potential of purifying saponins using a nanofiltration membrane. Increasing operating pressure caused the flux to increase and the decreased rejection value. The flux of pure saponin feed was greater but generated lower rejection rates than the saponin-BSA feed.

Increasing feed concentration resulted in an increased rejection rate. However, the flux decreased with increasing pure saponin concentration but increased with a higher dose of saponin-BSA. The DSS-ETNA01PP membrane had the largest flux value and the smallest rejection value compared to other membranes. The results indicated that nanofiltration was potential for the saponin purifying process.

Acknowledgements

The authors would like to thank the Membrane Research Center (MeR-C), Integrated Laboratory, Diponegoro University for funding this research.

References

Augustin, J. M.; Kuzina, V.; Anderson, S. B.; Bak, S, 2011. Molecular Activities, Biosynthesisand Evolution of Triterpenoidsaponins, *Phytochemistry*, 72, 435–457.

Bart, H.J. Extraction of natural products from plants—An introduction. Industrial scale natural products extraction, 1st ed.; Wiley-VCH: Verlag, 2011; pp. 1–26.

Carvalho, A.I.; Maugeri, F.; Pradanos, P.; Silva V.; Hernandez A, 2011. Separation of potassium clavulanate and potassium chloride by nanofiltration transport and evaluation of membranes, *Separation and Purification Technology*, 83, 23-30.

Chaiyasut, C.; Tsuda T, 2001. Isoelectric Points Estimation of Proteins by Electroosmotiv Flow: pH Relationship Using Physically Adsorbed Proteins on Silica Gel, *Chromatography*, 22(2).

Giichi, H. 1987. *Production of saponin containing no isoflavone from soybean embryo bud*. JP Patent 62,005,917.

Guclu-Untundag, O.; Mazza, G, 2007. Saponins: Properties, Applications and Processing. *Critical Reviews in Food Science and Nutrition*, 47, 231–258.

Hostettmann, K.; Marston, A. Saponins (Chemistry and Pharmacology of Natural Products). Cambridge University Press: Cambridge, 1995.

Kensil, C. A.; Marciani, D. J. 1991. *Saponin adjuvant*. US Patent 5,057,540.

Kezwon, A.; Wojciechowski, K., 2014. Interaction of Quillaja bark saponins with food-relevant proteins. *Advances in Colloid and Interface Science*, 209, 185-195.

Kitagawa, I. 1986. *Method of isolating soya saponins*. US Patent 4,594,412.

Lin, C. J.; Rao P.; Shirazi, S, 2004. Effect of operating parameters on permeate flux decline caused by cake formation – a model study, *Desalination*, 171, 95-105.

Norman, L.N.; Fane, A G.; Winston Ho, W.S.; Matsuura T. Nanofiltration. In Advanced Membrane Technology and Applications; John Willey & Sons, Inc., New Jersey, USA, 2008, pp. 271

Nozomi, O.; Haruo, S.; Shisai, R.; Fuku, S.; Hikari, J.; Toshi, H.; Bunshi, K. 1986. *Saiko saponin*. JP Patent 61,282,395.

Pedebos, C.; Pol-Fachin, L.; Pons, R.; Teixeira, C.V.; Verli, H., 2014. Atomic Model and Micelle Dynamics of QS-21 Saponin. *Molecules*, 19, 3744-3760.

Sparg, S. G.; Light, M. E.; van Staden, J., 2004. Biological activities and distribution of plant saponins. *Journal of Ethnopharmacology*, 94, 219–243.

Salgin, S.; Salgin, U.; Bahadir, S., 2012. Zeta Potensials and Isoelectric Points of Biomolecules: The Effect of Ion Types and Ionic Strenghts. *International Journal of Electrochemical Science*, 7, 12404 – 12414.

Susanto, H.; Stahra, N.; Ulbricht, M., 2009. High performance polyethersulfone microfiltration membrane having high flux and stable hydrophilic property. *Journal of Membrane Science*, 342, 153-164.

Sutzkover-Gutman, I.; Hasson, D.; Semiat, R.; 2010. Humic substances fouling in ultrafiltration processes. *Desalination*, 261(3), 218-231.

Takeuchi, T. M.; Pereira, C. G.; Braga, M. E. M.; Maróstica, M. R.; Leal, P. F.; Meireles, M. A.A. 2009. Low-pressure solvent extraction (solid–liquid extraction, microwave assisted, and ultrasound assisted) from condimentary plants. In M. A. A. Meireles (Ed.), Extracting bioactive compounds for food products—Theory and applications (pp. 140–144). Boca Raton: CRC Press, 151-158.

Vongsangnak, W.; Gua, J.; Chauvatcharin, S.; Zhong, J. -J., 2004. Towards efficient extraction of notoginseng saponins from cultured cells of Panax notoginseng. *Biochemical Engineering Journal*, 18, 115–120.

Wei, J.; Helm, G.S.; Corner-Walker, N.; Hou, X., 2006. Characterization of a non-fouling ultrafiltration membrane. *Desalination*, 192, 252-261.

Wu, J.; Lin, L.; Chau, L., 2001. Ultrasound-assisted Extraction of Ginseng Saponins from Ginseng Roots and Cultured Ginseng Cells. *Ultrasonics Sonochemistry*, 8, 347–352.